GL-TR-90-0172

AD-A227 425

JOULE HEATING INVESTIGATIONS USING THE SØNDRESTROM RADAR AND DMSP SATELLITES

Jürgen Watermann
Odile de la Beaujardière

SRI International
333 Ravenswood Avenue
Menlo Park, California 94025-3493

June 1990

Final Report
10 December 1989 — 9 May 1990

GEOPHYSICS LABORATORY
AIR FORCE SYTSTEMS COMMAND
UNITED STATES AIR FORCE
HANSCOM AIR FORCE BASE, MASSACHUSETTS 01731-5000

"This Technical report has been reviewed and is approved for publication"

FREDERICK J. RICH
Contract Manager

NELSON C. MAYNARD
Branch Chief

FOR THE COMMANDER

(DEPUTY)

for RITA C. SAGALYN
Division Director

This report has been reviewed by the ESD Public Affairs Office (PA) and is releasable to the National Technical Information Service (NTIS).

Qualified requestors may obtain additional copies from the Defense Technical Information Center. All others should apply to the National Technical Information Service.

If your address has changed, or if you wish to be removed from the mailing list, or if the addressee is no longer employed by your organization, please notify GL/IMA, Hanscom AFB, MA 01731. This will assist us in maintaining a current mailing list.

Do not return copies of this report unless contractual obligations or notices on a specific document requires that it be returned.

REPORT DOCUMENTATION PAGE

Form Approved
OMB No. 0704-0188

1. AGENCY USE ONLY *(Leave Blank)*	2. REPORT DATE	3. REPORT TYPE AND DATES COVERED
	1990 June	Final Report: 12/10/89–5/9/90

4. TITLE AND SUBTITLE
Joule Heating Investigations Using the Søndrestrom Radar and DMSP Satellites

5. FUNDING NUMBERS
PE 61102F
PR 2311 TAG5 WUBC
Contract: F19628-87-K-0006

6. AUTHOR(S)
J. Watermann, O. de la Beaujardière

7. PERFORMING ORGANIZATION NAME(S) AND ADDRESS(ES)
SRI International
333 Ravenswood Avenue
Menlo Park, CA 94025

8. PERFORMING ORGANIZATION REPORT NUMBER
Final Report
SRI Project 3083

9. SPONSORING/MONITORING AGENCY NAME(S) AND ADDRESS(ES)
Geophysics Laboratory
Hanscom Air Force Base
Massachusetts 01731-5000

Contract Manager: F. Rich/PHG

10. SPONSORING/MONITORING AGENCY REPORT NUMBER
GL-TR-90-0172

11. SUPPLEMENTARY NOTES

12a. DISTRIBUTION/AVAILABILITY STATEMENT
Approved for public release;
Distribution unlimited

12b. DISTRIBUTION CODE

13. ABSTRACT *(Maximum 200 words)*

The objective of our study was to cross-validate Joule heating rates derived from Defense Meteorological Satellite Program (DMSP) F7 observations through comparison with incoherent scatter radar measurements from Søndre Strømfjord, Greenland. In spite of obvious difficulties encountered within localized and dynamic structures such as discrete auroral arcs, where electric field and Pedersen current estimates did not match, good agreement was found within relatively stable structures like the poleward edge of the diffuse aurora. Unrelated to spatial and temporal ambiguity problems, a systematic discrepancy in the summer daytime Pedersen conductance calculations from spacecraft and radar data was found. Although the conditions for comparison were generally not optimal because the temporal and spatial coincidences between spacecraft and radar measurements were not perfect, 50% of the cases examined were in good agreement. Possible error sources for the remaining cases of disagreement are identified and explanations for the disagreement are offered. The necessity of further efforts to cross-validate measurements of ionospheric parameters is emphasized and ways for improvements of the comparison method are suggested.

14. SUBJECT TERMS	15. NUMBER OF PAGES
Ionosphere, auroral zone, electric fields, Pedersen conductance, Pedersen current, Joule heating	52
	16. PRICE CODE

17. SECURITY CLASSIFICATION OF REPORT	18. SECURITY CLASSIFICATION OF THIS PAGE	19. SECURITY CLASSIFICATION OF ABSTRACT	20. LIMITATION OF ABSTRACT
Unclassified	Unclassified	Unclassified	SAR

CONTENTS

LIST OF ILLUSTRATIONS

LIST OF ILLUSTRATIONS, CONTINUED

I INTRODUCTION

The purpose of this study is to validate and calibrate a technique of calculating Joule heating* rates from measurements made by low altitude, earth orbiting satellites. This is done by comparing the results from satellite data with those from simultaneous measurements from a high-latitude incoherent scatter radar. The effect of the Joule dissipation on the neutral atmosphere has far reaching consequences. It causes upwelling of the atomic oxygen which is then transported to lower latitudes; it changes the global configuration of thermospheric neutral winds (Roble et al., 1977; Prolss, 1980). It enhances the neutral density in the lower ionosphere through upwelling of the atmosphere. Therefore, the Joule heating rate is one of the most fundamental parameters in studies of the coupling mechanisms between the solar wind and the thermosphere-ionosphere-magnetosphere system. As a consequence, a number of studies were published during the last decade which attempted to determine height integrated Joule heating rates. Various combinations of observations and models were used (see, for example, Rich et al. [1989] for a brief review of the relevant studies). Thus it is highly desirable to cross-validate the results obtained with different methods to make them reliable and more useful.

In principle, the Joule heating rate q is a parameter describing the dynamics of the lower E region, and is computed from the dot product of electric field $\underline{E}$ and electric current density j:

$$q = \underline{j} \cdot \underline{E} = \underline{j}_{\parallel} \cdot \underline{E}_{\parallel} + \underline{j}_{\perp} \cdot \underline{E}_{\perp} \quad (W/m^3) \quad . \tag{1.1}$$

The symbols for parallel and perpendicular refer to the direction of the undisturbed geomagnetic field which can be approximated very well by an eccentric dipole some 500 km displaced from the center of the earth (Cole, 1963). It is generally assumed that parallel electric fields are negligible in the ionospheric E and F regions because the electron number density and parallel mobility is sufficiently high to short circuit electrostatic potential differences along the field lines. Thus the Joule heating rate reduces to

$$q = \underline{j}_{\perp} \cdot \underline{E}_{\perp} = \sigma_P E^2 \quad , \tag{1.2}$$

with $E^2 = \underline{E}_{\perp}^2$ and σ_P denoting the Pedersen conductivity. The Hall current is perpendicular to the electric field and, if gradient free, does not contribute to Joule heating.

---

*With the term "Joule heating" we refer to an energy transfer from the ion bulk motion to the thermal energy of ions and neutrals through collisions.

Integration over the lower ionosphere where ion-neutral collisions are important (typically between 90 and 250 km altitudes) gives the height-integrated Joule heating rate

$$Q = J_P E = \Sigma_P E^2 = \frac{1}{\Sigma_P} J_P^2 \quad (W/m^2) \tag{1.3}$$

with J_P denoting the height-integrated Pedersen current density and Σ_P the height- integrated Pedersen conductivity, i.e., the Pedersen conductance.

The measurements of Joule heating rates by incoherent scatter and satellite observations rely on the validity of several assumptions, namely, a certain model of the neutral atmosphere, and an ionospheric electric field perpendicular to the geomagnetic field and scaling in altitude as the geomagnetic field. Further assumptions that must be made but that differ for the two approaches are discussed in detail in subsequent sections.

Observations from satellites with suitable orbits make it possible to sample a wide range of latitudes in a short time and to provide an averaged global picture of Joule heating rates. However, because satellites cannot be steered to a certain location at a certain time to make observations related to a particular event, and because they cannot be held fixed at a certain position, it is not possible to resolve unambiguously questions involving spatial or temporal variations.

Ground-based radars, on the other hand, probe a fixed region in the ionosphere extending several degrees in latitude and longitude, but in principle they can do so at any given time, and for arbitrary long periods of time.

Thus, space borne and ground-based measurements of relevant parameters provide complementary data and thereby help to complete a picture of global and event related ionospheric Joule heating. However, it is important to ensure that both data sets and the methods used to infer Joule heating rates from the measured physical parameters will lead to consistent and comparable results. Therefore, a project was carried out with the objective to investigate the consistency of both methods and, in particular, to validate Joule heating rates inferred from satellite data while the satellite was moving through the field of view of the Sondrestrom incoherent scatter radar.

During the active phase of the project, the Defense Meteorological Satellite Program (DMSP) F7 satellite was the only continuously monitored spacecraft that could provide an estimate of the Joule heating rate. The F7 satellite was equipped with precipitating ion and electron detectors as well as a vector magnetometer (Hardy et al., 1979; Rich, 1984, Rich et al., 1985) and was flying at a virtually constant altitude of about 830 km in an almost polar sun-synchronous orbit with its ascending node at 1030 local time.

To calculate the Joule heating rate from satellite observations, the Pedersen conductance Σ_P is inferred from estimates of the ionospheric electron density produced by solar UV and EUV radiation, plus a contribution produced by the observed downward flux of energetic auroral electrons. The Pedersen current J_P is considered to be solely fed by field-aligned currents which at satellite altitudes are inferred from magnetometer recordings. The Joule heating rate is calculated from these two parameters.

The Sondrestrom incoherent scatter radar facility (further on in this report referred to as SSF), located on the west coast of Greenland at about 74° invariant magnetic latitude, is at most times within the auroral oval or the polar cap, which allows a direct calculation of the Joule heating rate in the polar ionosphere. The plasma density profiles and F region ion velocities are measured directly as a function of magnetic latitude. The Pedersen conductivity is calculated assuming a model ion-neutral collision rate, and the electric field is derived from the Hall drift of the F region ions. Both parameters are then combined to provide the Joule heating rate. Details of the methods are given in the following sections.

From this brief outline of the methods, it is clear that the results presented here may bear great significance. If the two entirely different methods (which have very little in common) lead to essentially the same results, we have an excellent confirmation of the validity of both methods and the utility of the assumptions and approximations made therein. This report will show that the two independent methods provide similar, but not always the same results. Occasional disagreement between both methods emerged mainly for two reasons: a systematic discrepancy was found, in the ionospheric conductances owing to solar UV and EUV radiation, and the highly localized and dynamic structures of the discrete aurora permitted reliable comparisons only if the observations were made sufficiently close in space and time. This was not the case for the majority of events available for analysis. However, for a number of events, there was good agreement, at least within part of the latitude range covered by both instruments.

II METHODOLOGY

II.1 DERIVATION OF PEDERSEN CONDUCTANCE, PEDERSEN CURRENT, AND JOULE HEATING RATE FROM DMSP-F7 MEASUREMENTS

The method used to derive height-integrated electric conductivity, Pedersen current, and Joule heating rate in the ionosphere from DMSP measurements was described by Rich et al. (1987) and is repeated here for convenience.

The geomagnetic field is assumed to be uniform and vertical, and the parallel conductivity is infinitely large throughout the ionosphere. As a consequence, the parallel electric field vanishes, and the perpendicular electric field is height independent. Further on, it is assumed that the horizontal electric current is limited in altitude between the bottom (symbol B) and the top (T) of an ionospheric layer that is completely confined to altitudes below the spacecraft.

The problem is considered to be a restricted three-dimensional one such that vectors may have components in all three dimensions; however, spatial variations of all (scalar, vector, and tensor) physical quantities are permitted only in two dimensions.

A cartesian coordinate system is adopted with x parallel to the geomagnetic field (vertically down in the northern polar region), y pointing towards geomagnetic north and z towards geomagnetic east. The z direction is taken as the dimension without spatial variation.

The method of Rich et al. (1987) is based on the current continuity equation

$$\nabla \cdot \underline{j} = 0 \quad , \tag{2.1}$$

Ampere's law

$$\nabla \times \underline{b} = \mu_o \underline{j} \quad , \tag{2.2}$$

and Ohm's law

$$\underline{j} = \underline{\sigma}\, \underline{E'} \tag{2.3}$$

with $\underline{E}' = \underline{E} + \underline{u} \times \underline{B}_o$ and $\underline{u}$ the neutral wind velocity in the E region. Height integration of the continuity equation with $\partial/\partial z \equiv 0$ results in

$$j_x(x=T) - j_x(x=B) = \frac{\partial J_y}{\partial y} \quad , \tag{2.4}$$

with J_y denoting the height integrated current density in the y-direction. It is assumed that no current can penetrate the bottom side of the ionosphere. The topside current extends uniformly upward. Thus, with j_x (x=B) = 0 and j_x (x=T) = j_{FAC}, the field-aligned current density, one finds

$$j_{FAC}(y) = \frac{\partial J_y(y)}{\partial y} \quad . \tag{2.5}$$

Ampere's law applied to the altitudes above the ionosphere yields

$$j_{FAC}(y) = \frac{1}{\mu_o} \frac{\partial b_z(y)}{\partial y} \quad . \tag{2.6}$$

Combining (2.5) and (2.6) and integrating over y results in

$$J_y(y) = \frac{b_z(y)}{\mu_o} + C_1 \tag{2.7}$$

The y-component of the height-integrated Ohm's law is

$$J_y(y) = \Sigma_P(y)\, E'_y(y) - \Sigma_H(y)\, E'_z(y) \quad . \tag{2.8}$$

The Hall conductance is assumed to be independent of y, and horizontal variations in $\underline{B}_o$ and vertical variations in $\underline{u}$ are neglected. Faraday's law,

$$\nabla \times \boldsymbol{E} = 0 \quad , \tag{2.9}$$

then shows that the Hall term in (2.8) is independent of y such that (2.8) is reduced to

$$J_y(y) = \Sigma_P(y)\, E'_y(y) + C_2 \quad . \tag{2.10}$$

Combination of (2.7) and (2.10) now gives the Pedersen current in y-direction

$$J_{Py}(y) = \Sigma_P(y)\, E'_y(y) = \frac{b_z(y)}{\mu_o} + C \quad . \tag{2.11}$$

Equatorwards of the auroral zone the field-aligned currents as well as the perturbation magnetic field are assumed to be zero. Integration of (2.6) from the southern boundary of the auroral zonal (y=S) to an arbitrary y gives

$$\int_S^y j_{FAC}(\tilde{y})\, d\tilde{y} = \frac{b_z(y)}{\mu_o} - \frac{b_z(S)}{\mu_o} = \frac{b_z(y)}{\mu_o} \quad . \tag{2.12}$$

Thus the constant C in (2.11) represents that part of the northward Pedersen current that is not fed by field-aligned currents. If one assumes that no significant Pedersen currents exist equatorwards of the auroral zone, that constant part vanishes.

The model requires that the field aligned currents are balanced in pairs, i.e.,

$$\int_S^N j_{FAC}(\tilde{y})\, d\tilde{y} = \frac{b_z(N)}{\mu_o} = 0 \quad , \tag{2.13}$$

when integrating from south (y=S) to north (y=N) of the auroral zone. Otherwise the excess field-aligned current must be carried away by Pedersen currents north of the auroral zone and in the y-direction, i.e., across the polar cap, as can be seen from Equation (2.11). The assumption of a vanishing magnetic perturbation field in the polar cap imposes the constraint that the field-aligned currents on the same meridian must be balanced in pairs within the auroral latitudes.

The height-integrated Joule heating rate may be written in the various forms

$$Q = J_{Py}\, E'_y = \frac{1}{\Sigma_P}\, J^2_{Py} = \frac{1}{\Sigma_P}\, \frac{b_z^2}{\mu_o^2} \quad , \tag{2.14}$$

the last one of which is the form used by Rich et al. (1987). While b_z is obtained from the difference between the magnetic field directly observed with an onboard magnetometer and an estimated background field, Σ_P is obtained in an indirect way. A recent paper (Rich et al., 1989) uses an improved method of deriving the perturbation magnetic field in the auroral oval.

Three sources of ionospheric ionization are assumed to be effective: the direct solar UV and EUV radiation, cosmic rays and background EUV, and the precipitation of energetic (auroral) electrons downward along the field lines. The solar-radiation produced term of the conductance is calculated from a formula given by Robinson and Vondrak (1984), with the 10.7 cm solar radio flux at 1 AU and the solar zenith angle as the governing parameters. A constant term of 0.1 mho is added to represent ionization from the background sources (Wallis and Budzinski, 1981). A modified formula is used for solar zenith angles close to 90°. The conductivity caused by energetic auroral electron precipitation is calculated after Robinson et al. (1987). This calculation assumes that the electron distribution is a Maxwellian.

II.2 DERIVATION OF IONOSPHERIC ELECTRIC FIELD, PEDERSEN CONDUCTANCE, AND JOULE HEATING RATE FROM INCOHERENT SCATTER RADAR MEASUREMENTS

The method used to infer the ionospheric electric field, Pedersen conductance, and Joule heating rate from incoherent scatter observations is quite different from the method described above for DMSP measurements. The observations are made by sending a pulse of 1290 MHz radio waves into the ionosphere. The ionospheric plasma scatters part of the pulse energy back to the radar station.

The height-integrated conductivities are derived from electron density profiles measured during the radar scans in the geomagnetic meridian plane. The computation requires that a neutral atmosphere model is specified. Comparisons of calculations based on the Banks and Kockarts (1973) and the MSIS-83 (Hedin, 1983) models show that the results are not particularly sensitive to the choice of a model. However, Brekke and Hall (1987) have pointed out that discrepancies between several conductance values published may be attributed in part to the choice of the ion collision frequency, i.e., the choice of a model.

A monostatic radar provides the line of sight Doppler velocity component from which the ionospheric electric field is obtained. Since the electric field is strictly perpendicular to the geomagnetic field, the electric field east component is estimated directly, knowing the

antenna elevation angle, when the radar beam is in the meridian plane. If we assume electric field invariance along the L-shells, the electric field may be derived from observations with the antenna pointing to the side (east and/or west) out of the magnetic meridian plane, which is essentially the principle of the multiposition radar mode. It is difficult to obtain reliable $E_\perp$ estimates close to the radar location, where the antenna beam is virtually aligned with the geomagnetic field.

Because the ion-neutral collision rate is low in the F region, the ion bulk motion is approximately not linked to the neutral air motion. The electric field derived from the F region ion bulk velocity does not contain a Lorentz term $\underline{u} \times \underline{B}_0$, which introduces a small error into the electric field comparisons. Using a method outlined in de la Beaujardière et al. (1977), a combination of E and F region measurements can be used to determine the electric field.

The two parameters, Pedersen conductance and electric field, lead directly to the height-integrated Joule heating rate:

$$Q = \Sigma_P E^2 \quad . \tag{2.15}$$

Under the assumptions stated, the Joule heating rate is only found as a function of latitude. In the following sections, we will study the variation of ionospheric parameters with geomagnetic latitude. In comparing radar and satellite observations, we normally used radar observations taken in the "World Day" mode, in which the radar is operated in an alternating sequence of elevation scans in the magnetic meridian and a set of four or five pairs of positions at different latitudes held fixed for some time. For a number of experiments, an extra position with the antenna beam pointing along the magnetic field line was added. Each observation cycle required between 5 and 50 minutes.

The electric field can be calculated independently from the elevation scan and from the multiposition part of the antenna cycle, the latter being generally more reliable.

The World Day mode provides the option to interpolate the electric fields from two multiposition cycles to the time of the spacecraft pass if ionospheric conditions prove to be sufficiently stable. When conditions are unstable, the electric field measurements from one set of multipositions or from the elevation scan closest in time to the satellite pass are used.

II.3 SOFTWARE DEVELOPMENTS

The standard program used to process radar elevation scan measurements, known under the name BLEDEN, provides the following quantities: electron density profiles along the magnetic field lines, Hall and Pedersen conductivities, and north and east components of

the electric field and of the electric currents. An option to merge data from elevation scans and multiposition cycles was added to the program. For each latitude, the electric field estimates from the multiposition data obtained before and after an elevation scan are interpolated to the time of the elevation scan when the radar beam at F region altitude reached the corresponding latitude. These electric field values are then combined with the conductance computed from the elevation scan data to give current densities and Joule heating rates.

There are two reasons for averaging the electric fields obtained from two consecutive multiposition cycles and merging them with elevation scan density measurements. First, the conductivities from the elevation scan are obtained with much finer resolution than those from the multiposition cycle which are obtained only over a very coarse latitudinal grid. Second, it is important to obtain the electric field as accurately as possible because the Joule heating rate is proportional to the square of the electric field. Under stable ionospheric conditions, the electric field obtained from multipositions is more reliable than that from elevation scans. By averaging over two multiposition cycles, the statistical accuracy is improved. The merged data are subsequently stored on magnetic tape in the so-called Export Format which has been adopted for the National Center for Atmospheric Research (NCAR) data base.

A new program, named EXPO, that was developed and added to the software package is a general purpose plotting routine that accesses data files written in the Export Format. EXPO plots series of any pairs of parameters, e.g., integrated conductivity versus invariant latitude, elevation scan electric field versus multiposition cycle electric field, etc. It is possible to display more than one series of data pairs in the same plot frame, e.g., northward current versus invariant latitude and eastward current versus invariant latitude.

Figure 1 illustrates the routine data flow through the different stages of data processing, from the on-line data acquisition to the final customized parameter display. A detailed description of the software used to process the radar data can be found in de la Beaujardière et al. (1980). Another modification of the software permits us to derive particle mobilities and thus conductivities not only from the Banks and Kockarts (1973) atmosphere model but also from the MSIS model (Hedin, 1983). For the cases tested, the difference between Pedersen conductance based on one or the other model was small.

To allow use of the existing higher level radar processing software for the DMSP data, an interface program was written that reads the DMSP data tapes, calculates additional geophysical parameters which are not contained in the tapes (electric field, current, and conductance), rotates the coordinate system if necessary, and reformats both the DMSP data and the derived quantities, into the Export Format. Thus, the existing plot programs can as well be used for the DMSP data to facilitate visual comparison.

The figures in the following sections display the physical quantities, from ground and space, in geomagnetic coordinates into which the electric field components were

transformed. In most of the figures which display SSF data a dotted line indicates positions where the line of sight was close to parallel with the geomagnetic field (blind spot overhead). In these positions, no reliable electric fields can be obtained.

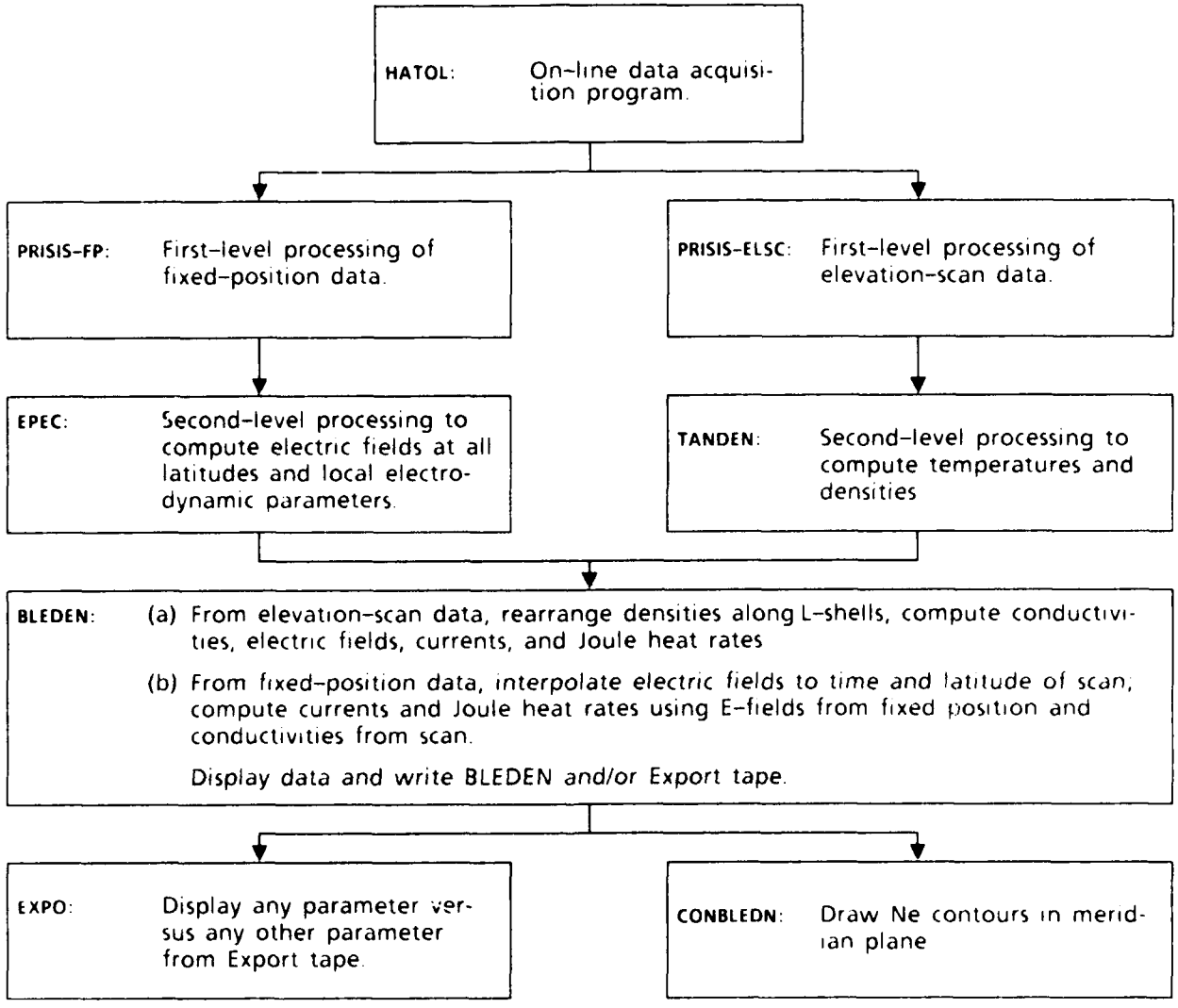

FIGURE 1. FLOW OF DATA ANALYSIS PROGRAMS

III COMPARISON OF INDIVIDUAL EVENTS

We now turn towards a comparison of individual coincident DMSP/SSF observations, which we refer to as "events." After having defined the conditions which were used to select these events, we will discuss them in more detail.

In order to be considered as an event for our comparison, a DMSP pass over Sondre Stromfjord should take place under as many as possible of the following conditions:

1. The satellite orbit is as close as possible in geomagnetic longitude to the radar site, so as to eliminate errors resulting from misalignment between L shells and the structure of the auroral zone (boundaries, field-aligned current sheets, auroral arcs).

2. The auroral zone structure is stable over several minutes to tens of minutes, so as to reduce interpretation uncertainties that may result from temporal variations of the aurora because it takes a few minutes for the radar to scan in elevation along the magnetic meridian plane.

3. The radar field of view is located in the auroral oval and not in the polar cap. The DMSP method of Joule heating estimation is only applicable to the auroral oval.

4. Significant field-aligned currents are detected when the satellite is within the radar field of view since the DMSP method hinges on measurements of the magnetic perturbation resulting from field-aligned currents.

5. The radar is operating in a mode that contains elevation scans in the geomagnetic meridian so as to measure a latitudinal profile of the E region electron density. This is needed to derive the latitudinal variation of electric conductivities. A sequence of alternating elevation scan and multiposition cycles is desirable for better estimates of the electric field.

We have identified 11 passes of the DMSP-F7 satellite over Sondre Stromfjord which meet the selection criteria reasonably well to enable us to perform a comparison between ground and space data. The following table lists the DMSP passes selected for comparison.

Table 1
DMSP-F7 PASSES SELECTED FOR COMPARISON WITH RADAR OBSERVATIONS

Day	Date	UT	EL	χ	ΔB	Radar Mode	Remarks
84 067	07 Mar	1134	65	77.8	400	WD	Pass examined by Tsunoda et al. (1985)
84 151	30 May	1203	83	53.6	1000	WD	Oval and small cusp signature
84 180	28 June	1225	79	53.7	1500	WD	Oval field-aligned current pair
84 195	13 July	1227	78	56.3	600	WD	Oval to the south, cusp overhead
84 282	08 Oct	1151	75	86.3	700	AZ and EL	Oval overhead, cusp north
85 015	15 Jan	1216	85	92.4	300	WD	Unique current sheet? Good temporal coincidence
85 016	16 Jan	1156	79	93.8	300	WD	Unique current sheet?
85 179	28 Jun	1238	68	52.6	800	EL	Cusp and unique oval sheet?
85 197	16 Jul	1135	72	61.3	300	WD (modified)	
86 268	25 Sep	1224	69	79.4	500	WD	Multiple current sheets
86 269	26 Sep	0208	63	119.2	200	WD	Only example around midnight

The columns denote (from left to right): year and day of year; date; Universal time of DMSP-F7 being seen from the radar under highest elevation; corresponding elevation angle; solar zenith angle at that time; maximum magnetic disturbance measured on the spacecraft while crossing the auroral oval; radar mode with WD = World Day mode (alternating elevation scan and multiposition cycle), AZ = azimuth, EL = elevation scan, WD (modified) = World Day plus field-aligned fixed position.

Only one out of the 11 events was a night pass, because the Sondrestrom radar, located at a high invariant latitude, is observing the polar cap instead of the auroral oval during most nights. Nevertheless, this event is an important one because it does not contain any solar radiation produced ionization and thus eliminates one model input parameter, namely, the Robinson and Vondrak (1984) term of the height-integrated conductivities.

In the following subsections we discuss the 11 listed coincident DMSP-F7/SSF events in more detail. We do not repeat everything contained in the eight quarterly status reports submitted between April 1987 and January 1990; rather, we attempt to present a concise and systematic evaluation.

III.1 EVENT 840307

The DMSP pass occurred during times of relatively stable geophysical conditions. A radar elevation scan along the magnetic meridian nearly coincided in time with the satellite pass, which was displaced by 300 km to the magnetic east of SSF. The electron density contour plot for the elevation scan (Figure 2) shows to the south an enhanced E layer density which is probably related to diffuse aurora, and auroral precipitation produced ionization with a peak at 150 km altitude about 140 km north of SSF. Figure 3 displays electric field components, Pedersen conductances, and Joule heating rates inferred from both DMSP and SSF. Note that the SSF derived Σ_P is only available over 3° latitude since it is mainly determined by the lower E region electron population where SSF has only a narrow field of view. Because the SSF electric field is derived from F region plasma velocities, it is obtainable over a wider range. To achieve a better match between SSF and DMSP, the SSF data were shifted southwards by 0.75° which corresponds to a 15° misalignment between auroral structure and local L-shell. Such a misalignment is quite possible and indeed is often observed.

While the DMSP and SSF electric fields are in good, although not excellent, agreement, provided we take the 0.75° latitudinal shift into consideration, the agreement of the Pedersen conductances is not satisfactory. Conductance falls off from a peak of 9 mho at the radar latitude to about 3 mho at 1° north of the radar in both the DMSP and SSF data; however, south of the radar at 73° latitude, the DMSP conductivity is still between 7 and 8 mho and only gradually declining, while the SSF conductivity shows a decrease to only 4 mho, about half of the DMSP value. The Joule heating rates match well poleward of 74°, but not equatorward. At latitudes below 74.5°, the SSF Joule heating is larger than that of DMSP, despite the significantly smaller SSF Pedersen conductance. It indicates that the larger SSF electric field overcompensates the smaller SSF conductance, which is understandable from the fact that the squared electric field enters the formula to calculate Joule heating.

III.2 EVENT 840530

Ionospheric conditions appeared to be unstable during the hour preceding the overpass, as indicated by a sequence of latitudinal electric field profiles. The four panels of Figure 4 show the SSF electric field components derived from an elevation scan about 30 min before the SSF pass (a), from two multiposition cycles before and after that elevation scan and interpolated to the time of the elevation scan (b), and from an elevation scan

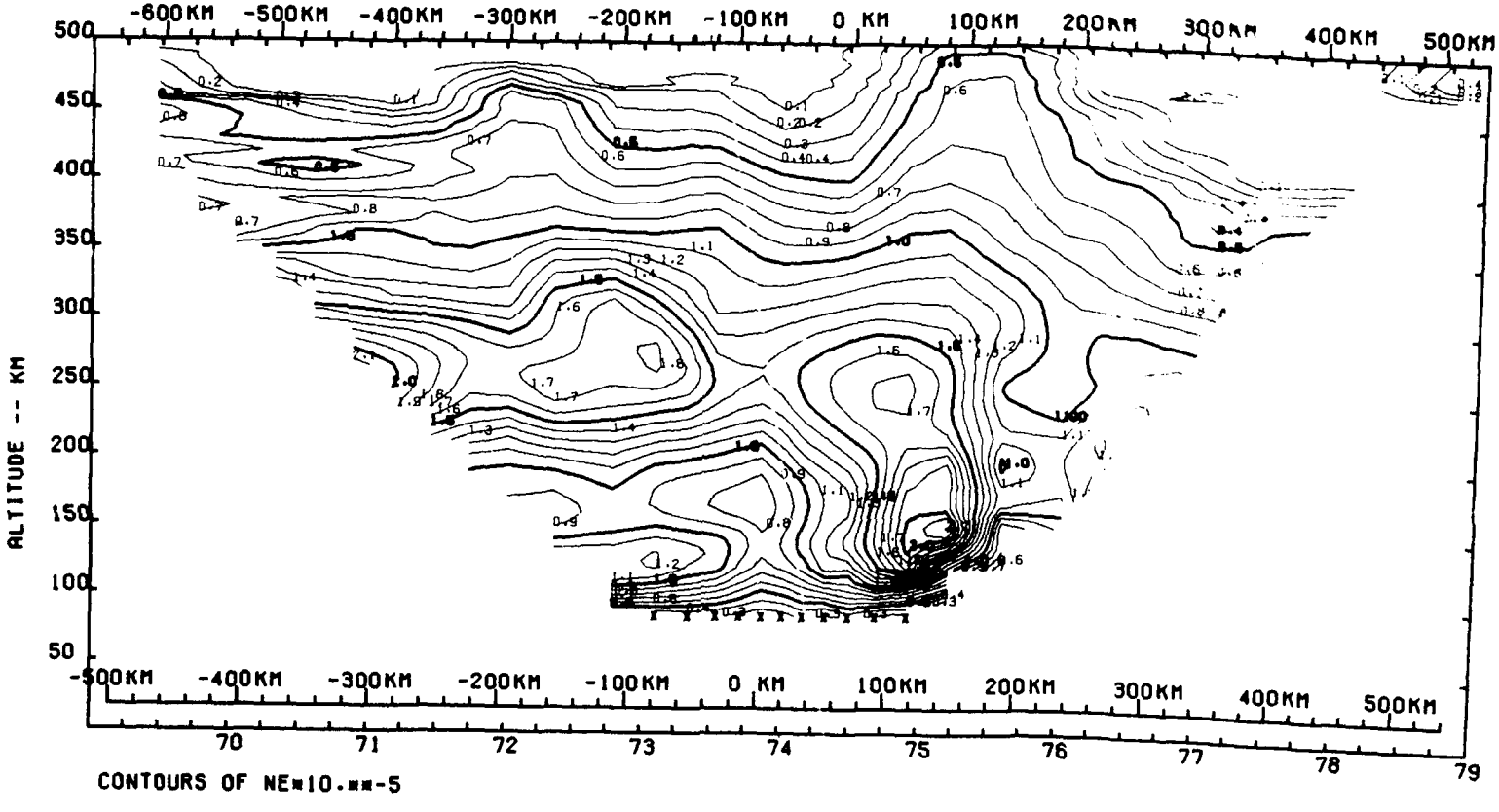

FIGURE 2 ELECTRON DENSITY CONTOURS IN THE GEOMAGNETIC MERIDIAN FOR THE 1132-1137 UT SCAN, 7 MARCH 1984

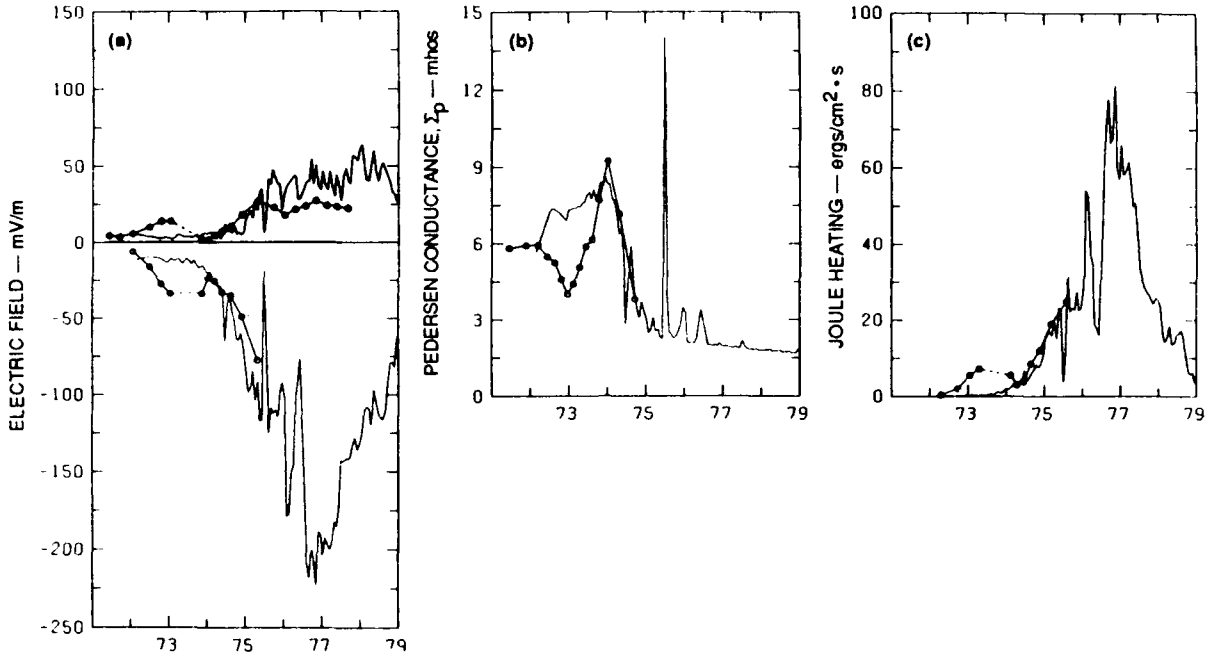

FIGURE 3 ALMOST SIMULTANEOUS OBSERVATIONS FROM THE DMSP-F7 SATELLITE (SOLID LINES) AND THE SØNDRESTRØM RADAR DURING AN ELEVATION SCAN (SOLID LINES WITH CIRCLES) ON 7 MARCH 1984, AROUND 1135 UT

(a) Electric field east (thin) and north (heavy) components. (b) Pedersen conductances. (c) Joule heating rates. Closest approach was 300 km horizontal distance, the Søndrestrom profiles are shifted to the south by 0.75° to compensate for misalignment between constant invariant latitude contours and auroral structures.

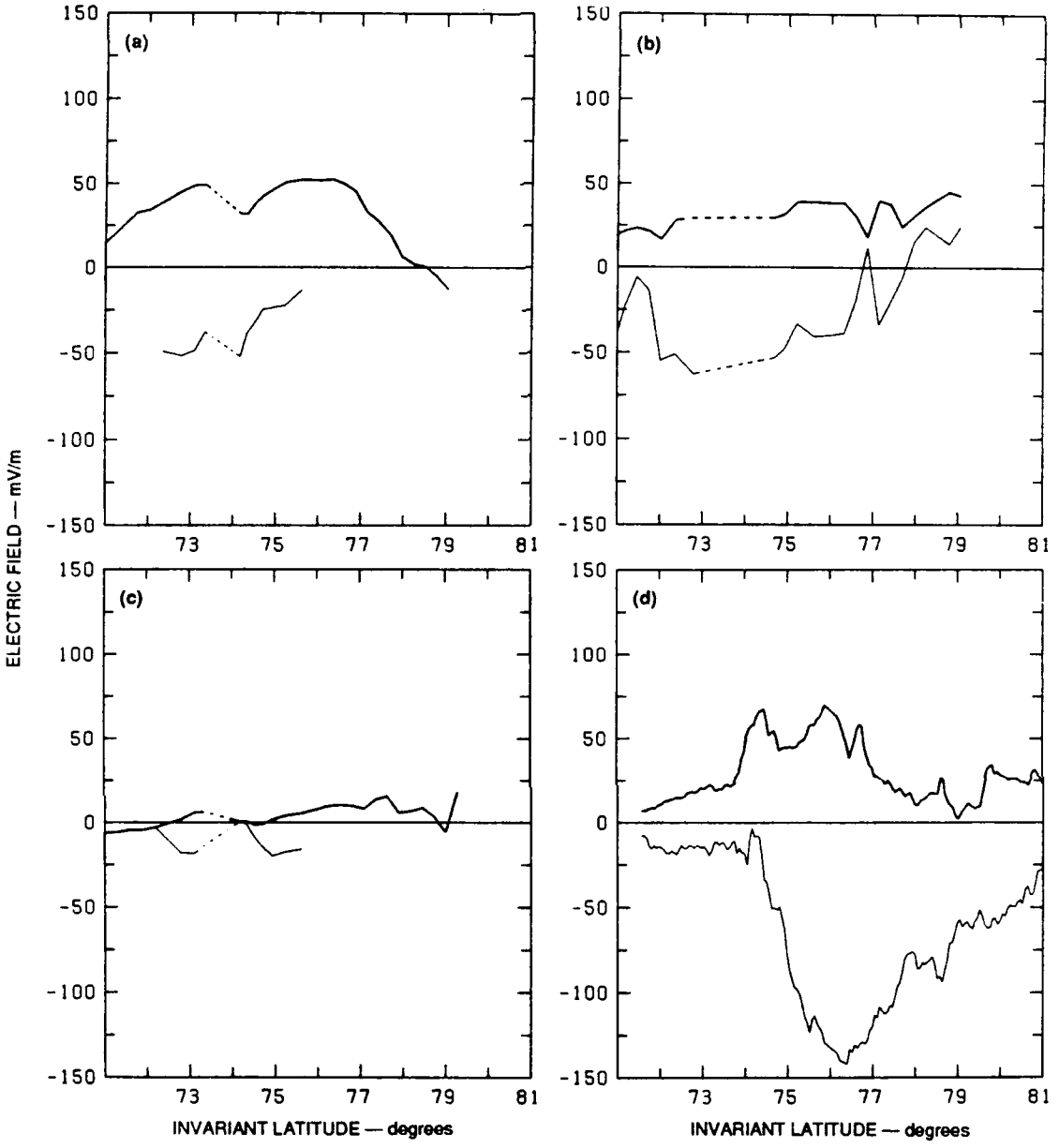

FIGURE 4 ELECTRIC FIELD COMPONENTS IN THE EAST (X) AND NORTH (Y) DIRECTIONS FOR THE DMSP PASS OF 30 MAY 1984

(a) Sǿndrestrom radar data from the elevation scan before the DMSP pass. (b) Sǿndrestrom data from the multiposition measurements interpolated to the time of the elevation scan before the pass. (c) Sǿndrestrom data from the next scan, just after the DMSP pass. (d) DMSP-derived data. Heavy line indicates north component; light line incidates east component. The Sǿndrestrom blind spot is indicated by the dotted segments.

immediately after the DMSP pass (c). Therefore, it is not surprising that the DMSP electric field (d) does not match well with any of these, except that the signs of the north (heavy line) and east (thin line) components are consistent. The auroral activity was low during this time, with only low energy particle precipitation; thus the conductances reflect mainly the solar radiation produced ionization and change very little with latitude (see Fig. 5a). The agreement is within about 15% and is good. The Joule heating rates (Fig. 5b) do not agree because of the mismatch in the electric fields. Although this event cannot be considered to be a success for the cross-validation of the two methods, its results are explained in terms of temporal variation of the ionosphere around the time of the satellite pass and the relatively long time needed to run a full radar observation cycle.

III.3 EVENT 840628

A temporal sequence of SSF electron density profiles indicates fairly stable conditions in the ionosphere. But substantial differences exist between DMSP and SSF measurements (not shown). The peak amplitude of the DMSP electric field reached more than 200 mV/m between 76° and 76.7° and was virtually southward oriented while the SSF multiposition electric field changed from some 80 mV/m south-southeast at 76° to some 35 mV/m eastward at 76.7°.

Latitudinal Pedersen conductance profiles derived from SSF data and DMSP show mainly solar radiation produced ionization north of SSF and a little additional precipitation-produced ionization south of SSF (see Figure 6). The DMSP Pedersen conductance is systematically higher than the SSF value by about 30%. A comparison of Joule heating rates reveals total disagreement owing to the poorly matching electric fields. We will return to the systematic discrepancy in Σ_P later.

III.4 EVENT 840713

The DMSP pass over Sondre Stromfjord corresponds to very low particle flux which did not contribute significantly to the ionization of the lower E region. However, the ionization produced through solar radiation during this event at 0900 local time, close to summer solstice, ensured the nonnegligible Pedersen conductance shown in Figure 7, together with the value inferred from the radar. As in event 840628 (Section III.3), the slight slope in the DMSP curve indicates the variation of ionization with varying solar zenith angle; again the DMSP value is systematically higher than the SSF value, in this case by about 50%. If all the assumptions for applying the method outlined in Section II were valid, the electric field inferred from the DMSP magnetometer should be systematically smaller than the SSF-measured field. This was not the case; the two seemed to have nothing in common, neither the orientations nor the zero crossings. However, this is not surprising because the DMSP pass took place during a time of change in the electric field and convection pattern, as can be seen from Figure 8. The line at 1220 UT, indicating the DMSP pass, falls between two

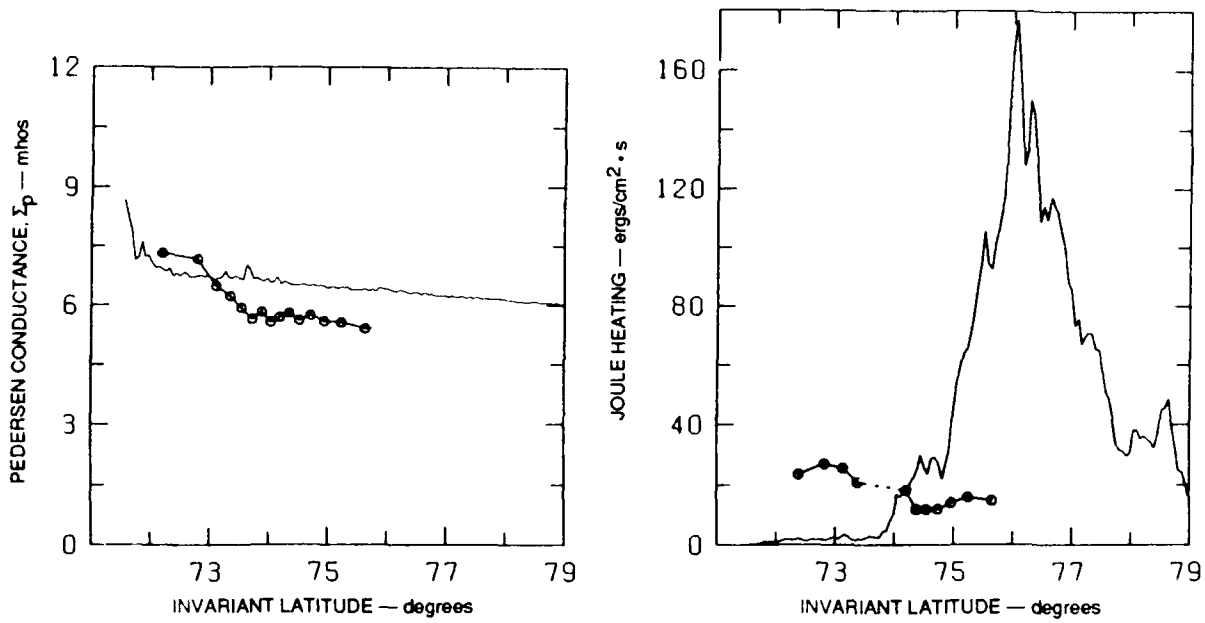

FIGURE 5 PEDERSEN CONDUCTANCE AND JOULE HEATING RATE DERIVED FROM DMSP MEASUREMENTS (SOLID LINE) AND THE SØNDRESTROM ELEVATION SCAN BEFORE THE DMSP PASS (LINE WITH CIRCLES) ON 30 MAY 1984, AROUND 1200 UT

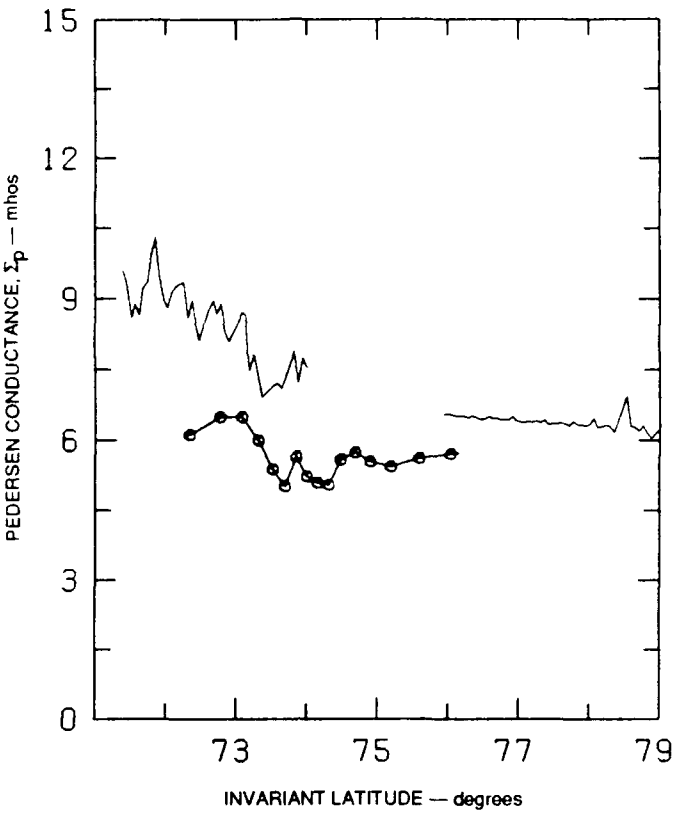

FIGURE 6 PEDERSEN CONDUCTANCE FROM DMSP (SOLID LINE) AND SØNDRESTROM ELEVATION SCAN (SOLID LINE WITH CIRCLES) MEASUREMENTS ON 28 JUNE 1984, SHORTLY AFTER 1200 UT

A gap appeared in the DMSP data used for the plot between 74° and 76°invariant latitude. Inspection of data received later filling in the gap showed a virtually monotonic decrease of Σ_P over the gap.

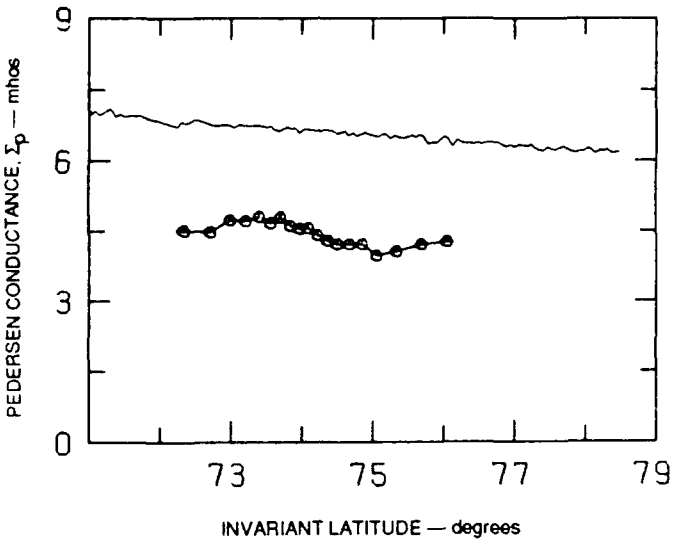

FIGURE 7 PEDERSEN CONDUCTANCE DURING THE DMSP PASS OVER SØNDRESTROM ON 13 JULY 1984, AROUND 1225 UT

Because of very low particle flux, Σ_P reflects mainly the solar zenith dependence of ionization through solar radiation.

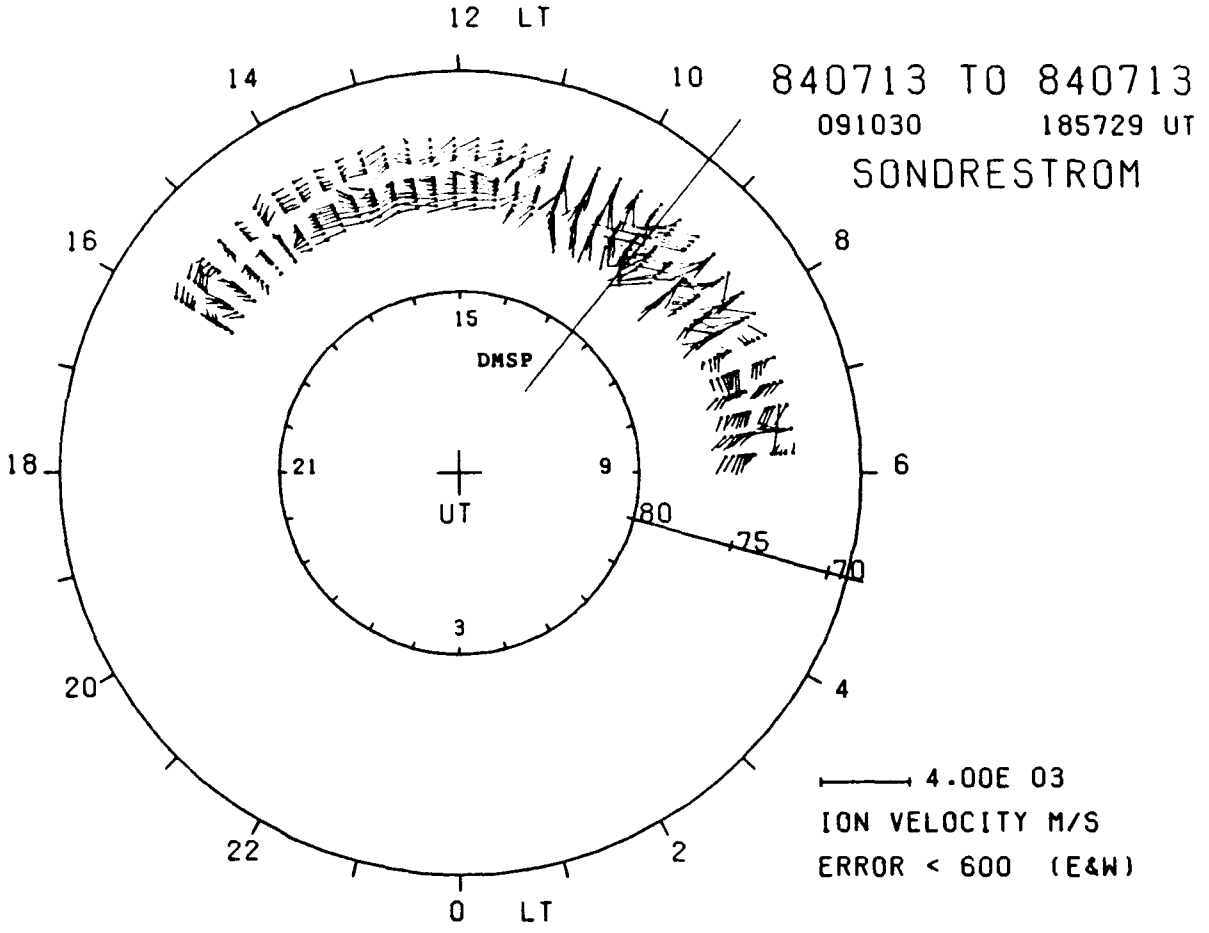

FIGURE 8 PLASMA VELOCITY VECTORS OVER SØNDRESTROM ON 13 JULY 1984, AS FUNCTION OF INVARIANT LATITUDE (ALONG THE RADIUS) AND TIME

1200 local time (corresponding to 1500 UT) is at the top. The satellite overpass at 1220 UT is indicated by the line marked DMSP.

radar observation cycles that show a change in the ion convection pattern from predominantly northeast to predominantly northwest. This leaves the convection direction at the time of the DMSP pass pretty much undetermined. The Joule heating rates look very different as well, and we do not show their latitudinal profiles here. The important point in this example is rather the systematic discrepancy in the conductances derived from both methods.

III.5 EVENT 841008

In contrast to the event discussed in the previous subsection, this pass occurred after the fall equinox when the solar zenith angle at SSF is already large and the solar radiation produced low ionization. However, it was a time of considerable auroral activity. Figure 9a displays the average energy from precipitating electrons measured on board DMSP-F7 (for its definition see Rich et al., 1987). In many cases, the average energy is a much clearer indicator of the structure of the aurora and of the transition from diffuse to discrete than the total number flux or total energy flux. The southern part of the auroral oval is characterized by an extended diffuse aurora, which ends abruptly at 74.2° invariant latitude; in the northern part is a sequence of auroral arcs with increasing average energy. This pattern of auroral energetic electron precipitation determines the Pedersen conductivity shown in Figure 9b where the SSF data are overlaid on the DMSP data.

The electric field components fit fairly well, not precisely in amplitude but in their general trend (see Figures 9c and d). *In Figure 9, a shift in latitude of 1° to the north* was applied to the radar data. As already discussed in a previous section, the shift reflects a misalignment between the longitudinal extension of the auroral structures and the constant invariant latitude shells. Such an offset resulting from misalignment is possible since the spacecraft crossed the L-shell through SSF some 200 km east of the radar site. The radar electric fields shown in Figures 9c and 9d were taken from an elevation scan some 10 minutes before the overpass. The next scan, some 10 minutes after the pass, showed less good agreement, the major mismatch owing to a change of sign in the north component. The Joule heating rates from both scans and from the satellite overpass in between were in fair agreement as can be seen in Figure 9e. This example shows that even in complex structures such as a combination of diffuse and discrete aurora the two methods agree reasonably well if (i) the ionospheric structure remains temporally stable so as to permit comparison between both data sets and (ii) we shift the radar data systematically in latitude to allow for a misalignment between local L-shell and arc structure.

III.6 EVENT 850115

The DMSP average energy plot of electron precipitation indicates the presence of a diffuse aurora in the south with its northward edge around 75° invariant latitude, and a discrete arc at 76.7°. Since the SSF solar zenith angle is large in January the DMSP

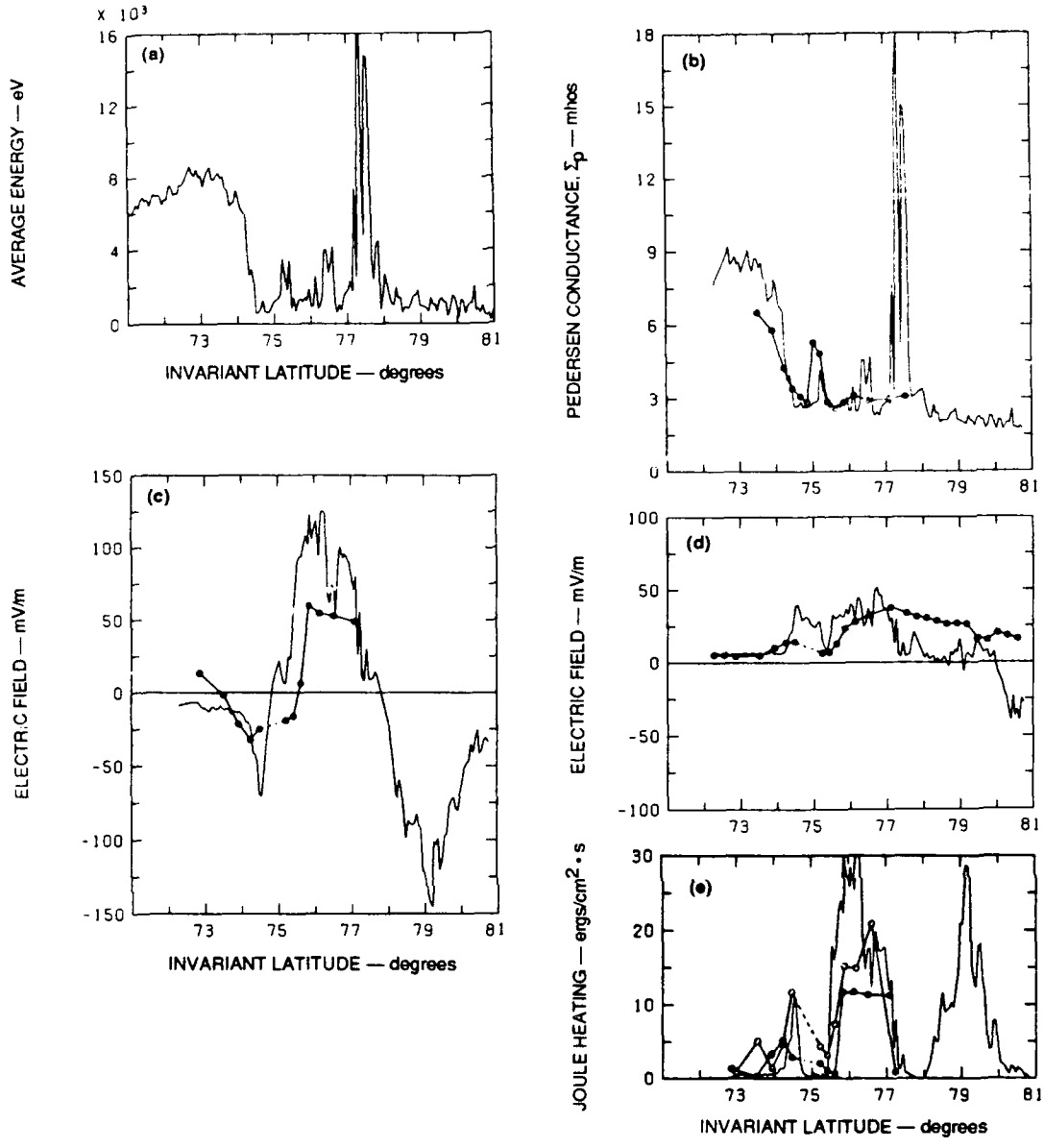

FIGURE 9 IONOSPHERIC PARAMETERS DERIVED FROM DMSP (SOLID LINES) AND SØNDRESTROM (LINES WITH CIRCLES) OBSERVATIONS ON 10 OCTOBER 1984, AROUND 1150 UT

(a) Average energy of auroral electron flux observed on DMSP-F7. The southern part up to 74.2° invariant latitude represents diffuse aurora precipitation, between 75° and 78°three discrete arcs with substructures can be identified. (b) Pedersen conductance estimated from the DMSP satellite (solid line) and the Søndrestrom elevation scan preceding the pass (line with circles). The Søndrestrom profile is shifted by 1°to the north to compensate for misalignment between L-shell and diffuse aurora boundary. (c) Electric field north component derived from DMSP measurements (solid line) and the Søndrestrom elevation scan preceding the pass (line with circles), shifted to the north by 1°.
(d) Corresponding electric field east component (e)DMSP and Søndrestrom Joule heating rates for the same event, with the Søndrestrom profiles shifted toward the north by 1°. Open circles represent the elevation scan preceding the DMSP pass, full circles the scan succeeding the pass

inferred Pedersen conductance simply reflects the auroral ionization (see Figure 10). A sequence of electron density contour profiles derived from radar observations from half an hour before to half an hour past the DMSP pass indicates the steady development of a weak diffuse aurora south of about 74° and a growing auroral arc around 75° which slowly moved to the north. The SSF Pedersen conductance curve shows a corresponding peak at 75° and a slight enhancement of Σ_P south of the arc, in the diffuse aurora region. The weak and narrow arc close to 77° seen in the DMSP particle data was outside the E region field of view of the SSF radar.

The north components of the SSF and DMSP derived electric fields match reasonably well if offset by 15 mV/m; they coincide in their change of sign and show the same overall trend (not shown). However, the east components do not match as well. At lower latitudes (below 75°) they are both small (less than 15 mV/m) but with different orientations, and between 75° and 77° they tend to diverge considerably. Thus one cannot expect to find well matching Joule heating rates, which proved to be true.

III.7 EVENT 850116

The DMSP pass took place during a time of rapidly changing geomagnetic conditions. The electric fields measured by the radar were fairly intense and variable around the time of the satellite pass (1153-1158 UT). During the elevation scan closest in time to the satellite pass (1204-1208 UT), the electric field pattern was very different from that derived from DMSP observations. However, a close examination of the radar data before the satellite pass shows that a much better agreement between the measurements is obtained using radar data from the multiposition cycle and the elevation scan before the pass, even though the time separation between those radar observations and the DMSP pass becomes larger.

The DMSP particle data indicate a transition from diffuse to discrete aurora at 73.5° invariant latitude with the diffuse aurora being characterized by high particle average energy up to about 6 keV. The discrete aurora with an average energy below 2 keV is not expected to contribute much to the Pedersen conductance. Since the event occurred in the northern hemisphere winter the solar radiation did not contribute significantly, and the Pedersen conductance profile (see Fig. 11b) simply reflects the auroral average energy profile. The SSF latitudinal Σ_P profile, overlaid on the DMSP profile in Fig. 11b, differs in that it shows two clearly distinct peaks. When shifted poleward by 0.25°, these peaks appear at 73.3° and 74.4°, and the northern flank of the lower latitude peak coincides with the edge of the diffuse aurora in the DMSP pattern. The two SSF maxima are clearly detected as maxima in the electron density contour plots. The southern peak virtually at the southern edge of the radar E region field of view may represent the poleward edge of the diffuse aurora while the northern maximum is believed to correspond to a discrete arc. Our interpretation is supported by the fact that the southern peak remained quite stable over consecutive radar

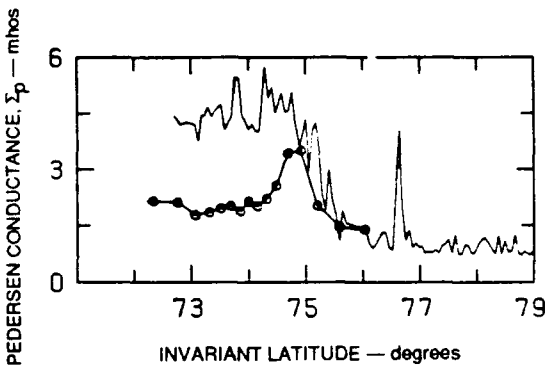

FIGURE 10 PEDERSEN CONDUCTANCE FROM DMSP OBSERVATIONS (SOLID LINE) ON 15 JANUARY 1985, AROUND 1215 UT, AND CORRESPONDING SØNDRESTROM MEASUREMENTS (LINE WITH CIRCLES)

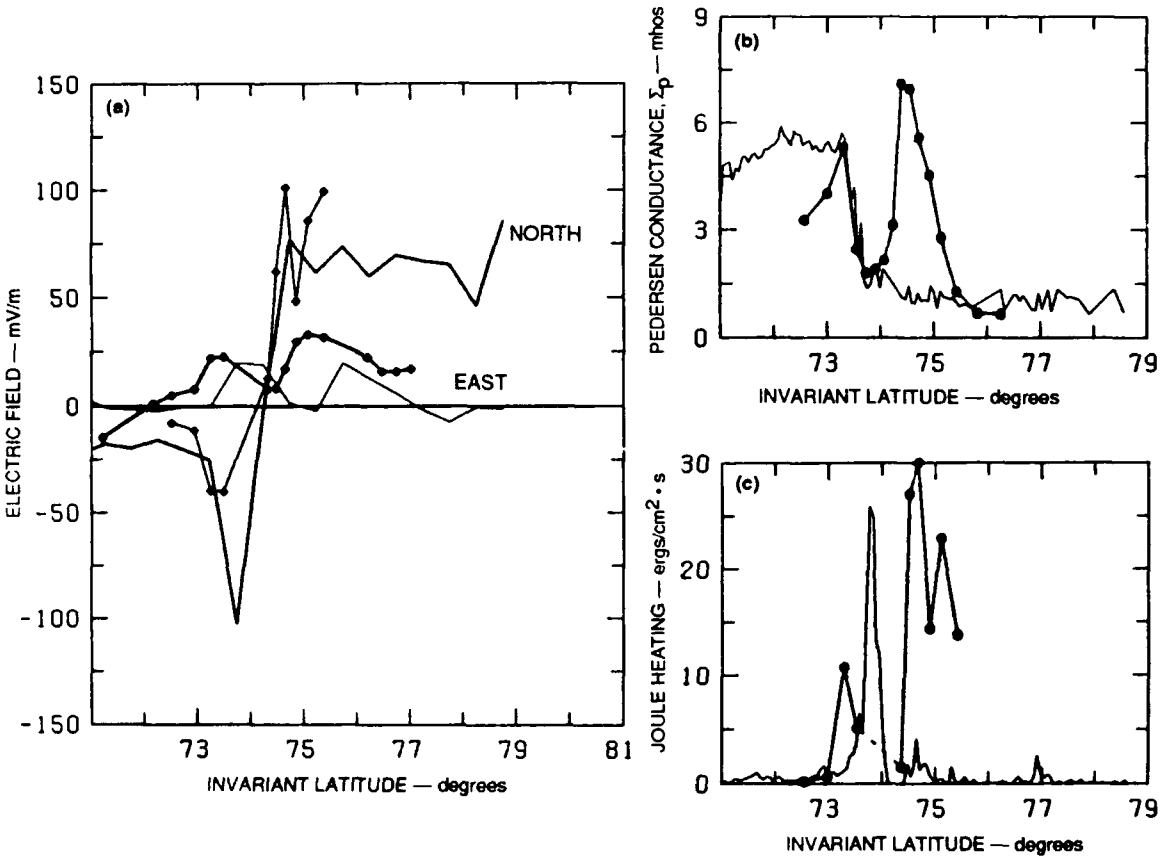

FIGURE 11 IONOSPHERIC PARAMETERS FROM DMSP (SOLID LINES) AND SØNDRESTROM (LINES WITH CIRCLES) OBSERVATIONS ON 16 JANUARY 1985

(a) Electric field north and east components. (b) Pedersen conductance. (c) Joule heating rates. The DMSP electric fields were averaged over 0.5°, the Søndrestrom profiles are shifted poleward by 0.25°.

scans while the northern peak amplitude changed with time, which is typical for discrete auroral arcs.

The electric fields, Figure 11a, show remarkably similar patterns--the same trends, zero crossings, and orientations--when the 0.25° poleward shift of the SSF data is taken into account. For this plot the DMSP electric field data were averaged over 0.5° to smooth them for better comparison. In both data sets, the electric field north components show a southward maximum at the edge of the diffuse aurora and a reversal within the discrete aurora. However, the large southward amplitude of the DMSP measured Pedersen current between 73° and 74° correlated with the peak in the southward electric field determines the Joule heating rate between 73° and 74° while the larger SSF north and east fields at latitudes higher than 74.3° and the larger SSF Pedersen conductance determine the Joule heating in the northern part of the profile. Thus, Joule heating rates agree less well than would have been expected from the good electric field agreement (Figure 11c).

III.8 EVENT 850628

The plasma drift vectors are plotted in Figure 12 as a function of time and latitude. The flow intensity as well as the latitude of the flow reversal changed in the two radar profiles that bracket the DMSP pass. Therefore we do not expect a close agreement between the DMSP and SSF electric fields. Indeed, the east components do not agree very well, while the north components agree between 73.5° and 75.2° (see Figures 13a and b). The Sondrestrom values appear systematically higher, by an almost constant value, throughout the field of view, for both Ey and Ex. This shift could be caused by an offset in the DMSP magnetic field after correction of the DMSP data for the geomagnetic background field. We still find a similar pattern of Joule heating rates (Fig. 13c). The large SSF electric field around 75.8°, of course, corresponds to a high peak in the Joule heating rate. The DMSP measured Pedersen conductance (not shown here) exceeds the SSF value systematically by about 30%, but otherwise both of them follow the same trend. Note that the systematic discrepancy falls on a day close to the summer solstice, with much E layer photoionization.

III.9 EVENT 850716

The magnetic activity appeared to be low during the DMSP pass, such that a reliable magnetic perturbation field at the DMSP altitude was only available north of 76.5° invariant latitude. The SSF electric fields were also very small, and they agreed well with the DMSP derived electric fields. The DMSP particle detectors showed diffuse aurora south of 77°, but no precipitation north of it. DMSP measured Pedersen conductance data are also available only north of 76.5°, a region into which the SSF radar E region field of view does not extend. Therefore, no direct comparison of Pedersen conductances is possible. One may, however, argue that, owing to the low activity and the small solar zenith angle, the E

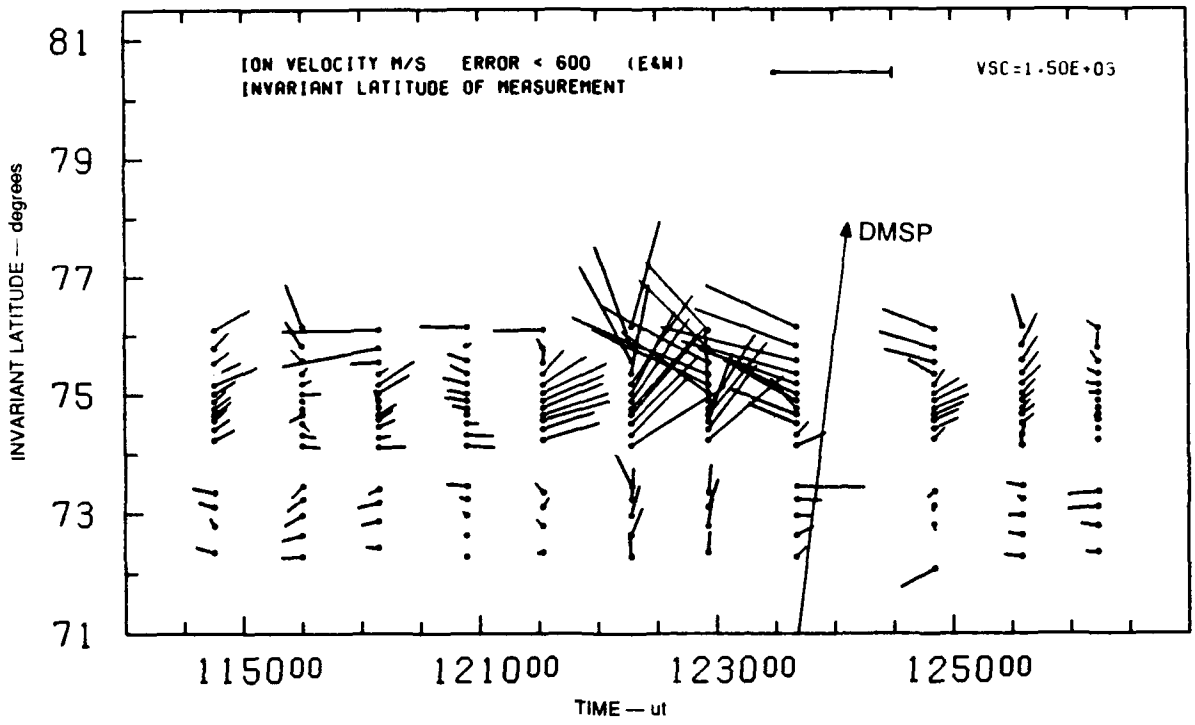

FIGURE 12 SEQUENCE OF ION VELOCITY PROFILES VERSUS INVARIANT LATITUDE MEASURED WITH THE SØNDRESTROM INCOHERENT SCATTER RADAR BETWEEN 1140 AND 1310 *UT ON 28 JUNE* 1985

The time-latitude track of the DMSP-F7 pass is indicated by the arrow. The DMSP pass occurred during a period of changing convection direction south of 75.2°.

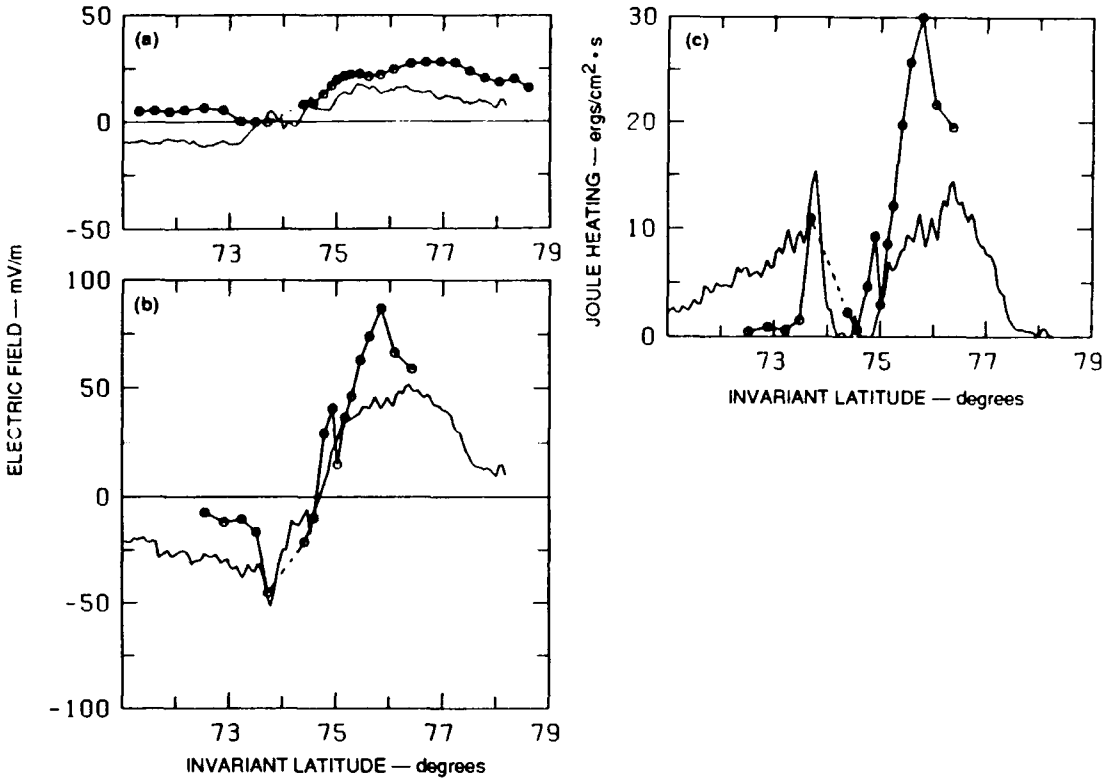

FIGURE 13 ELECTRIC FIELD AND JOULE HEAT RATE DERIVED FROM DMSP (SOLID LINES) AND SØNDRESTROM (LINES WITH CIRCLES) OBSERVATIONS ON 28 JUNE 1985, AROUND 1150 UT

(a) Electric field east components. (b) Corresponding north components. (c) Joule heat rates for the same event. The Søndrestrom profiles are shifted to the north by 0.25°.

region ionization north of 77° was mainly produced by solar radiation (see Figure 14). South of 77° one expects a higher conductivity because of the added influence of the diffuse aurora precipitation which was measured on DMSP with an average energy between 4 and 6 keV. The straight dashed line in Figure 14 represents extrapolation of the DMSP curve of Σ_P corresponding to the solar radiation is indicated by the straight dashed line in Figure 14. This line should be taken as the lower limit of the conductance since the auroral precipitation contribution to Σ_P has to be added. We have thus again an indication that the DMSP conductance systematically exceeds the SSF values shown between 72° and 76°. As before, we note that this discrepancy is seen at daytime in the summer.

Because of the nonoverlapping latitude regions between the various parameters measured, it is not possible to calculate and compare Joule heating rates for this event.

III.10 EVENT 860925

The DMSP particle data indicate a region of diffuse aurora south of 73° to 74° invariant latitude. The edge cannot be determined exactly since there appears to be a gap in the DMSP data. The SSF electron density profiles, covering the E region from about 72.5 to 75.5°, show a bright arc centered at 74.5° which may have been the same as seen by DMSP at 73.5 to 74°. Thus we may again have a misalignment between L-shell and arc structures. If the SSF profiles are shifted to the south by about 0.5° we find good agreement between DMSP and SSF Pedersen conductances within the arc and also outside of the arc where Σ_P reflects primarily the solar radiation ionization (see Figure 15, with the data gap interpolation dotted).

The electric fields measured during the SSF elevation scan shortly after the DMSP pass were virtually zero while the interpolation of two multiposition cycles, preceding and succeeding the elevation scan, were in agreement with the DMSP derived field, at least in the north component. Amplitude and orientation variations appear to coincide when allowing for a 0.5° south shift of the SSF data. The east electric fields are much weaker and agree less well; the SSF east component is small where the DMSP one is large, and vice versa. Since only the Pedersen conductances but not the electric fields are in good agreement between 72° and 75°, we find poor agreement in the Joule heating rates.

This event is another example in which the particle precipitation pattern (and thus Σ_P) seemed to be quite stable over a period of about 1 hour. The electric field pattern, however, changed quickly and significantly, thus making a comparison between Joule heating rates difficult.

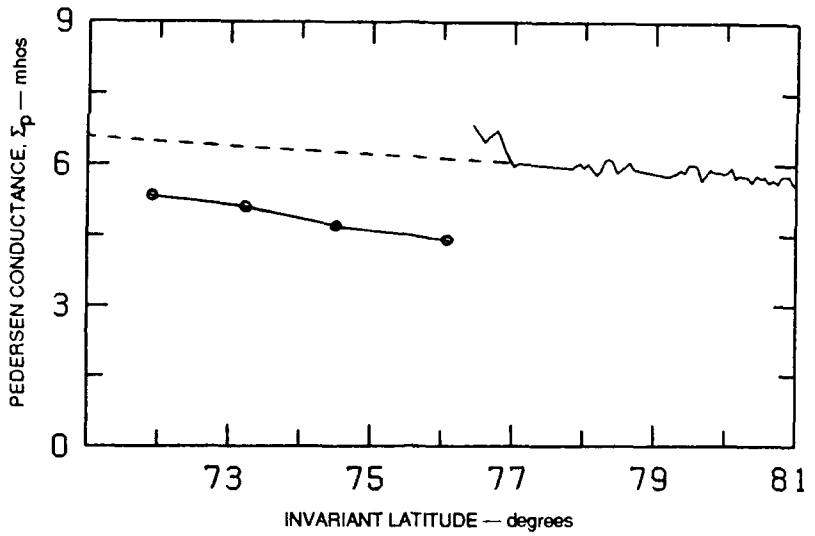

FIGURE 14 PEDERSEN CONDUCTANCE FROM DMSP (SOLID LINE) AND SØNDRESTROM (LINE WITH CIRCLES) MEASUREMENTS ON 16 JULY 1985, AROUND 1135 UT.

DMSP data of Σ_P were not available south of 76.5° invariant latitude. The dashed line indicates the extrapolation of the DMSP data when no ionization by energetic particles is assumed. Actually, diffuse aurora was observed south of 77°, which would raise the DMSP conductance to values above the dashed line.

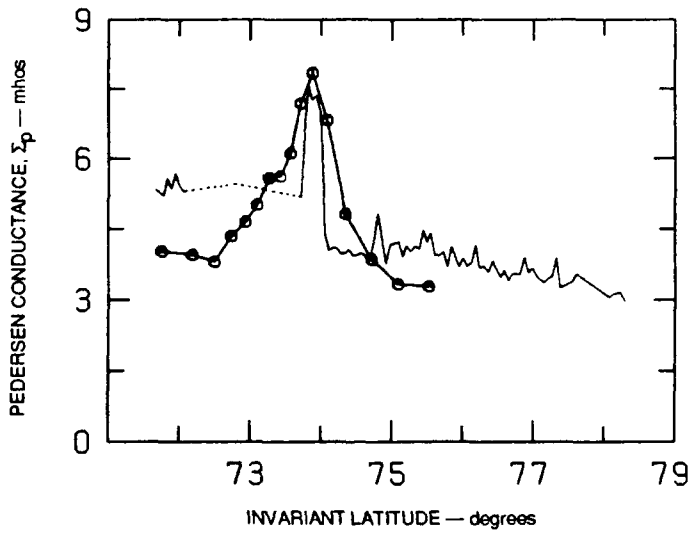

FIGURE 15 PEDERSEN CONDUCTANCE FROM DMSP (SOLID LINE) AND SØNDRESTROM (LINE WITH CIRCLES) MEASUREMENTS ON 25 SEPTEMBER 1986

The Søndrestrom profile is shifted to the south by 0.5°.

III.11 EVENT 860926

The event is a unique case because it is the only true night pass in our series of events. Concerning the E region ionization produced by solar radiation, the January 15/16, 1985, "daytime" passes around 0830 local time occurred while the solar zenith angle was larger than 90°. In that respect, the conditions were more night-like than day-like (see the solar zenith angles in Table 1). However, the pass at 2230 local time discussed in this section is close to midnight and thus possibly different from the winter morning passes.

The DMSP particle data indicate diffuse aurora extending up to about 73° invariant latitude followed by discrete aurora with several individual arcs between 73.7° and 75.2°. In the absence of solar radiation, Σ_P follows the auroral precipitation pattern. The electron density profiles measured by the radar show electron density enhancements corresponding to the DMSP particle flux increases, thus Pedersen conductances derived from both match excellently (see Figure 16c). Of course, the radar with its coarse multiposition grid cannot resolve details. The DMSP derived electric field components show distinct peaks around 73.6°, at the southern edge of the discrete aurora, and again at 75.2°, at its northern edge (see Figures 16a and 16b).

The SSF southward component peaks at 72.7° and appears to be small up to about 74.3°, but then increases again to reach a second peak at 75.2°, just as the DMSP field does. The DMSP and SSF westward components are very similar at southern latitudes, the region of diffuse aurora, and again, in the region of the north arc. However, when looking in between, both diverge. A close inspection reveals that the DMSP and SSF measurements actually may represent the same field. The DMSP east component peaks around 73.6° and falls into the SSF blind spot. The radar measurements close to the blind spot are the least reliable. Farther away from the radar, south of 72.5° and north of 74.3°, the electric field east components agree very well. A similar argument applied to the north components does not resolve the mismatch equally well, but one can at least argue that the peak in the DMSP southward component falls into the blind spot of the radar.

The Joule heating rates do not match well (see Figure 16d). At latitudes where either the Pedersen conductance is small (around 73.5°) or the electric field is small (around 74°) the DMSP and SSF-derived Joule heating rates are both small. Between 74.5 and 75° where enhanced electron density is noticed, the substantial difference in the southward electric fields corresponds to a large Joule heating difference.

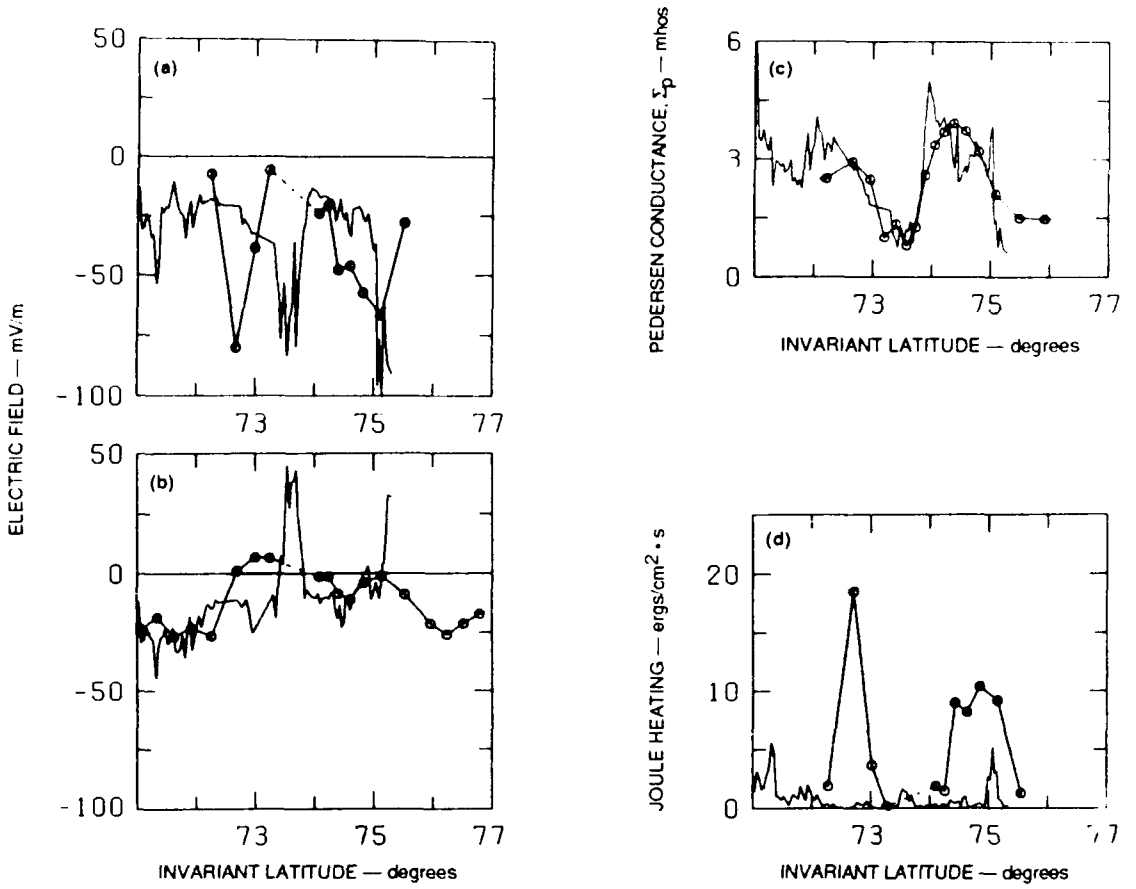

FIGURE 16 IONOSPHERIC PARAMETERS FROM DMSP (SOLID LINES) AND SØNDRESTROM (LINES WITH CIRCLES) OBSERVATIONS DURING THE NIGHT PASS—0200 UT OF THE SATELLITE OVER SØNDRESTROM ON 16 SEPTEMBER 1986

(a) Electric field North components. (b) East components. (c) Pedersen conductance. (d) Joule heating rates.

IV EVALUATION

IV.1 EVENTS

Although the number of events evaluated--11 between March 1984 and September 1986--and the varying solar and ionospheric conditions under which the data were taken yield no comprehensive data set, some important general results can still be obtained.

Our sample of events comprises one nighttime and 10 late morning passes of the DMSP-F7 satellite over Sondre Stromfjord, spread over all seasons but taken during a period of minimum activity in the 11-year solar cycle. For some of the events, the E region ionization was mainly solar radiation produced, in particular during the summer daytime passes. For other events that occurred under disturbed conditions, the ionization reflected mainly the auroral precipitation. The Pedersen conductivity is a direct manifestation of the ionospheric ionization, and the height-integrated Pedersen conductivity, Σ_P, is mainly dependent on the E region electron density profile.

The ionization pattern produced by solar radiation is of a global scale, thus we expect Σ_P values derived from DMSP and SSF data to be insensitive to a spatial separation of a few hundred kilometers. The general impression is, however, that Σ_P values from space and ground do not match very well with regard to solar radiation ionization. The DMSP values are systematically between 15% and 50% higher than the SSF values, with the largest discrepancy found at smallest solar zenith angles in the months of June and July (see Table 1).

Pedersen conductances primarily reflecting auroral particle precipitation agree well in some cases and less well in others. In contrast to the solar radiation, energetic auroral electron precipitation is a localized phenomenon which may in some cases extend only a few km or tens of km perpendicular to the auroral arcs. The orientation of the arcs may vary from event to event, which we tried to compensate by systematic northward or southward shifts of the SSF profiles. Furthermore, discrete auroral arcs tend to be very dynamic, and their fine structure may change significantly over a time interval of a few minutes. Since the events selected for our comparison were not optimal in the sense that, for most of them, a SSF meridional elevation scan (the mode providing electron density profiles) occurred several minutes before or after but not during the DMSP pass, and that during some events the spacecraft was displaced by several hundred km to the east or west from the radar site, we have to expect some disagreement. Indeed, we have seen in the SSF data that some spacecraft passes occurred just at a time of changing ionospheric conditions (see Figures 4, 8 and 12).

A failure of detecting discrete auroral arcs at the same latitude in DMSP precipitation and SSF electron density data is thus understandable in terms of varying ionospheric

conditions and cannot be considered a failure of the method. In some cases, it is not clear whether the radar detected an isolated auroral arc or just the edge of a precipitation region extended in latitude since the SSF field of view is only 3° wide in the E region. If we look at the transition from diffuse to discrete aurora, which is often seen over Sondrestrom when scanning in the meridian plane, we find fairly good agreement between DMSP and SSF data (see Figures 3, 9b, 10, 11b, 16). Note, however, that in some cases we had to allow for a misalignment between contours of constant invariant latitude and the poleward edge of the diffuse aurora and shift the SSF profiles accordingly.

It is encouraging to notice that these boundaries between diffuse and discrete aurora, which are generally more global and stable in time than individual arcs, were detected nearly coincidentally in the DMSP and the SSF data. An interesting phenomenon for which we presently have no explanation occurs systematically at the diffuse aurora poleward edge. The SSF Pedersen conductance does not simply fall off north of the diffuse aurora (except for discrete arcs) but mostly shows a distinct peak just at the edge of the diffuse aurora before taking on the lower values north of it (see Figures 3b, 10, 11b, 15, and 16c). Such poleward edge peaks are not usually present in Σ_p calculated from the DMSP data.

The most serious problem in our comparison concerns the electric fields. Since the electric field is squared for Joule heating computation, discrepancies between DMSP and SSF derived electric fields exaggerate the Joule heating discrepancy. Electric fields are not directly obtained by either instrument. The radar uses line-of-sight Doppler velocity components of the F region ion bulk motion. Measurements from different spots are merged and assumed to represent the same pure $\underline{E} \times \underline{B}_0$ drift, thus yielding the electric field components. The spacecraft uses the magnetic perturbation of field-aligned currents which are subsequently equated to meridional Pedersen currents. With the knowledge of the Pedersen conductance the effective electric field $\underline{E}' = \underline{E} + \underline{u} \times \underline{B}_0$ can eventually be derived. Because there are so many possible sources of errors involved, we cannot expect excellent agreement between radar $\underline{E}$ and spacecraft $\underline{E}'$. In addition, the ionospheric electric fields can be very localized and highly variable in time and thus very often evade direct comparison, even with perfect measurements, if they do not coincide in space and time.

Taking these difficulties into consideration, we need to emphasize that 50% of the events studied show rather good agreement. These are events 840307, 841008, 850116, 850628, 860926, and the north component of 860925. Very often a direct comparison of Joule heating rates is hampered by small scale spatial and temporal variations of the order of a few degrees in longitude and a few minutes in time. In these cases, we do not find satisfactory agreement between DMSP and SSF observations. However, we wish to emphasize that the mismatch cannot be considered a failure of the methods. It seems to be more a result of not having enough passes very close in space and time and simultaneous with radar measurements designed especially for the spacecraft overpass.

IV.2 METHODS

In the previous subsection, we have discussed how certain shortcomings in the observations and their mutual relation in time and space can contribute to a mismatch between space-based and ground-based derivations of the Joule heating rate. We have seen that the disagreement can in part be attributed to our incomplete knowledge about certain ionospheric processes, for example, the E layer ionization resulting from solar radiation, and in part to spatial and temporal separation between radar and spacecraft measurements. In this subsection we will discuss the methods used to derive Joule heating rates and the validity of their assumptions, and we will try to assess their impact on the results obtained.

As in the previous subsection, we first turn to the Pedersen conductance. The DMSP inferred Σ_P values were computed after an empirical formula based on the evaluation of data from 13 "quiet" days observed with the Chatanika radar during the time period 1972 to 1981 (Robinson and Vondrak, 1984). The data shown here indicate that the validity of this formula for the years 1984 to 1986 may be in doubt, which may explain some of the observed discrepancy.

An underestimate of the E region density derived from the radar may be another explanation. This, however, is not a likely explanation because, as we have already discussed, DMSP and SSF values of Σ_P match fairly well for stable auroral structures and for the diffuse aurora in particular. Furthermore, the Sondrestrom data are regularly calibrated by ionosonde measured densities.

The validity of the formula for the solar radiation produced conductance may be questionable, because this formula was derived from data of the preceding solar cycle at a different site. However, it was the only formula available making use of empirical data from the polar ionosphere under various solar flux levels. Other investigations used mostly data from only one day or two consecutive days. For a comparison of the different formulae see Table 1 in Brekke and Hall (1987). In a more recent paper, Rasmussen et al. (1988) included a dependence on the solar radiation level. Note that the Rasmussen et al. paper was not published at the time when the major part of the DMSP analysis was performed. Their formula is based purely on theoretical calculations and did not consistently agree with observations (de la Beaujardière et al., 1988). Application of their formula would have resulted in even higher estimates of the Pedersen conductance than the Robinson and Vondrak formula. Thus the use of the Robinson and Vondrak formula, together with the minor adjustments made and described in Rich et al. (1987) appeared to be the most reasonable and reliable choice. However, the data comparison between DMSP and SSF has revealed the urgent need to improve on the derivation of ionization produced by solar radiation. It may be that the 10.7 cm solar flux, one of the two controlling parameters in the formula (the other is the solar zenith angle) does not provide a good value of the solar radiation activity. Our findings are consistent with those of Barth et al., (1990), who showed that the ratio of Lyman-alpha radiation to 10.7 cm flux is much lower during solar minimum than during solar maximum.

The Robinson and Vondrak (1984) formula incorporated in deriving Joule heating rates from DMSP data relies on a square-root relationship between the cosine of the solar zenith angle and the height-integrated Pedersen conductivity. Other formulas use a linear relationship (Senior, 1980; de la Beaujardière et al., 1982); an approximately square root relationship (Mehta, 1978; Schlegel, 1988); an almost equally weighted mixture of both (Brekke and Hall, 1987); or even a dependence on the square of the normalized solar zenith angle (Rasmussen et al., 1988). These differences, however, can account for only 20% mismatch during summer noontimes at SSF and they would result in a larger discrepancy at large solar zenith angles. That is just the contrary of what we have seen in the data, which exhibit the biggest difference for the smallest solar zenith angles of the data set available. It rather seems that the estimation of Vickrey et al. (1981), based on Chatanika equinox to winter observations during solar minimum (1976/77), is more representative for our observations than the Robinson and Vondrak formula.

The auroral electron flux used to infer the Pedersen conductance is assumed to be isotropic. There is no way to test this hypothesis since the DMSP electron detector looked always to the zenith. However, it is known that this assumption is not necessarily valid. For example, electron flux observations made with the 1ESØ19 electron spectrometer on board Spacelab-1 in December 1983 at 250 km altitude in the southern auroral oval (Barrow et al., 1990) show a distinct enhanced electron flux level in a 30° cone which corresponds to a 25° cone at 830 km altitude. The spectra are reproduced in Figure 17. Since the pitch angle distribution influences the energy deposition rate in the ionosphere the isotropy assumption may contribute to errors in the conductance computation.

One assumption in the method used by Rich et al. (1987) concerns the north-south gradient of the Hall conductance, which is neglected in the estimation of the Joule heating rate. For the solar radiation component we have a slow variation with latitude for both, Σ_P and Σ_H, and a virtually constant ratio Σ_P/Σ_H. Thus a gradient free Σ_H is a reasonable assumption.

The situation may be different during auroral electron precipitation. Diffuse aurora and auroral arcs are often characterized by an elevated average energy of the downflowing electrons (see Figure 9a as a typical example). Since the formulae used to derive Pedersen and Hall conductances are closely related in the way Robinson et al. (1987) proposed it and Rich et al. (1987) employed it, a steep gradient in average energy and a steep gradient in Σ_P would multiply to result in an even steeper gradient in Σ_H [see Equation (14) of Rich et al. (1987)]. Thus a distinct spatial variability of Σ_P, as in the auroral precipitation regions, is inconsistent with a gradient-free Σ_H. The effect on Joule heating may be less severe since most Joule heating occurs in the region of soft electron precipitation.

The other parameters entering the formulae for Joule heating computation are the electric field (in the case of the method applied to SSF data) and the Pedersen current (in the case of the method applied to DMSP data). The approximation of field-aligned and Pedersen current sheets extended infinitely in east-west direction, which was invoked in the

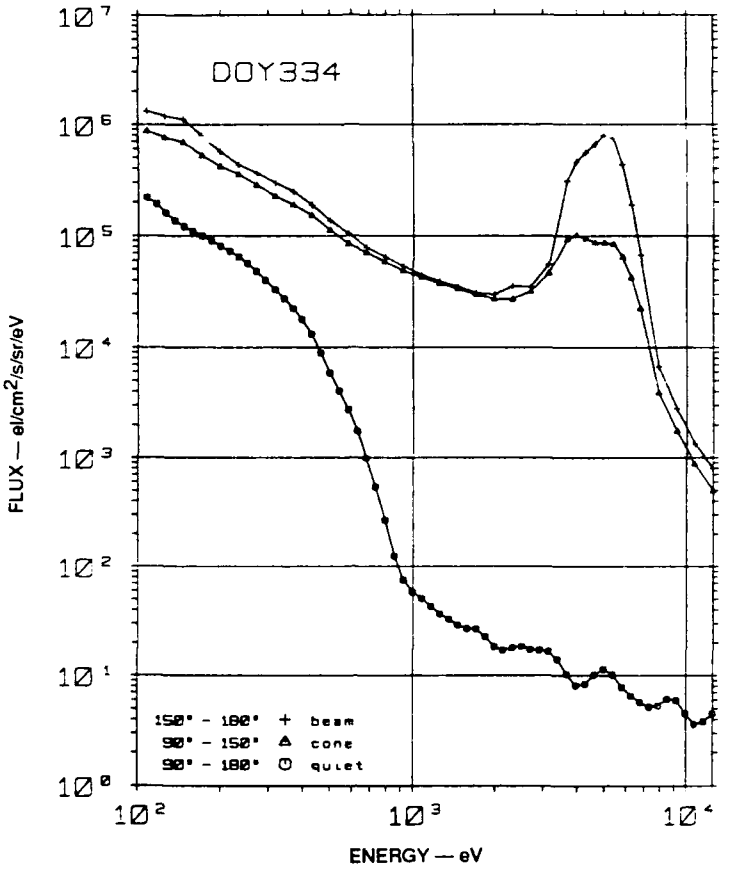

FIGURE 17 SUPERIMPOSED NUMBER FLUX SPECTRA OF AURORAL ELECTRON OBSERVATIONS FROM THE IES019 ELECTRON SPECTROMETER ON BOARD SPACELAB 1 ON 30 NOVEMBER 1983, AROUND 1942 UT

The space shuttle was at 96° longitude and –57° latitude (geographic) corresponding to –70° invariant latitude and approximately local magnetic midnight. Pitch angle ranges from 90° to 150° (indicated "cone") and 150° to 180° ("beam") with a characteristic energy of about 5 keV are compared with a background spectrum for 90°to 180° pitch angles obtained about 3 minutes later while Spacelab traversed a part of the polar cap.

method of Rich et al. (1987), does not consider eastward electric fields and Pedersen currents [see Section II, in particular, Equation (2.14)]. It is a very idealized approximation as was already noted by Rich et al. (1987). The real data have shown that varying eastward electric fields and currents exist and are not negligible in some of the events discussed. The uniformity along the z-axis (east direction), which was assumed in the derivation of the method in Section II.1, is often violated. However, this deviation from the ideal case is less disastrous than it may look at first glance. We simply define the coordinate system locally such that x is pointing downwards as before, y into the local direction of the horizontal electric field, and z completes the orthogonal right-handed system. Inspection of the DMSP method outlined in Section II.1 shows that the important equations establish either local or strictly height-integrated relations between the various physical parameters. However, the assumption about a global uniform structure of the auroral zone is no longer valid. It has two consequences: the field-aligned currents may not entirely feed into Pedersen currents and may not be balanced in pairs. The latter condition is expected to be violated in many cases anyway.

The ion bulk motion inferred from the radar spectra is derived from line-of-sight measurements. Several positions, i.e., several pointing directions of the radar are combined to provide a velocity vector perpendicular to the magnetic field. Thus a temporal and spatial stability of the ion convection pattern sufficient to permit merging of the data from several positions is required, which usually means a time interval of one or two minutes and a spatial extension of up to a few hundred kilometers in the F region. The ion bulk motion is transformed into an electric field via the $\underline{E} \times \underline{B}_0$ drift. In many cases the radar was operated in a mode with a cycle time too slow to provide a sufficient temporal resolution to follow the rapid variations of the electric field in the dynamic auroral ionosphere. The convection pattern may also vary on a scale considerably smaller than a few hundred kilometers, in particular during the highly localized auroral precipitation events.

The critical point is probably more a temporal variation than a spatial variation, because we have seen a number of examples with dynamic changes of auroral structures during a sequence of SSF radar scans. As far as the spatial variation is concerned, the electric field components often show a steady and continuous trend over several positions, except when the radar beam is close to alignment with the magnetic field. In the latter case, the line-of-sight component can be very erratic and provides a poor estimate of the velocity vector perpendicular to the magnetic field. To reduce the inherent uncertainty, radar positions on the same L-shell, but east and west of the radar location, should be included. Initially several DMSP passes over SSF were covered with radar operation especially designed for the purpose of this project. They might have provided data more suitable for comparison than those used for this report. Unfortunately, the corresponding DMSP data tapes were not kept and the data were not made available to us. Our study is therefore based on the analysis of retrospective data acquired under conditions that were not optimal.

Estimating the height-integrated Pedersen current from the observed magnetic perturbations which reflect field-aligned currents at spacecraft altitudes constitute another

problem. In order to extract the perturbation field from the three components of the absolute magnetic field measured on board DMSP, an IGRF model field and subsequently a hemispheric trend were subtracted. The trend was devised such that no perturbation field was allowed to exist in the polar cap, all perturbations were considered to be confined to the auroral region where field-aligned currents are expected.

Given the nature of the measurements and the lack of additional information during the DMSP passes, this method is, despite its uncertainties, probably the most reasonable way to derive the Pedersen current. In a recent paper, Rich et al. (1989) attempted to improve on it. Although the improvement is a step towards more sophisticated data analysis, it does not solve the problem in principle. Rich et al. (1987) noted that neglect of Hall currents may have a significant effect on the estimates of the Pedersen currents. As we have pointed out, an error in the Pedersen currents or the electric field, when raised to the exponent 2, will have an even larger effect on the Joule heating estimate.

To summarize, we believe that under the given circumstances the methods used for both DMSP and SSF data sets were the most reasonable way of analyzing, evaluating and comparing the data. We further believe that it is desirable to perform a comparison on data sets obtained with better coincidence in time and space and more appropriate radar operation modes.

V CONCLUSIONS AND RECOMMENDATIONS

One may think of several ways to cross-validate Joule heating rates estimated from spacecraft data. One way involves ground-based radar measurements. We have pursued it in this study in an attempt to validate the DMSP Joule heating computations. Using incoherent scatter radar observations, the ionospheric conductance is directly obtained from the measured electron density profiles and a model ion collision frequency. The results do not seem to be very sensitive to different neutral atmosphere models with slightly different collision rates. The electric field is inferred from the ion bulk motion under the assumption of a certain spatial and temporal stability needed to merge separately measured velocity components to calculate the velocity vector. Owing to a number of constraints in the available data sets, these two methods did not in general lead to an excellent agreement, although a number of individual events showed very promising and encouraging results. In particular, large scale patterns like the diffuse aurora poleward boundary turned out to match well.

In conclusion, we have obtained the following results:

(1) The method used to infer Joule heating rates from DMSP measurements is, under the given conditions, the most reasonable one. A number of events, in fact, more than 50%, show fairly good agreement with results from Sondrestrom *incoherent scatter radar.*

(2) There is still a certain amount of disagreement between both. Possible error sources have been identified and discussed.

(3) Directions for future work in order to arrive at better comparable Joule heating estimates have been pointed out. Further analysis of the solar produced conductivities, and well-planned coordinated measurements involving the Sondrestrom radar and the DMSP satellites have to be involved.

We recommend that the following studies be done to further validate and refine the method of calculating Joule heating from DMSP data:

1. Passes of suitable satellites should be selected which are closer in space than most of those discussed here. The optimal choice would be a spacecraft that passes over the radar site in magnetic north-south direction. Ideally, the satellite would be equipped with particle detectors, magnetometers and electric field probes. The radar would be operated in an elevation scan such that it follows the foot of the fieldline through the spacecraft as closely as possible in time. Such an experiment would resolve space/time ambiguities inherent in the data discussed here. It would be helpful to have more nighttime passes coincident with

radar observations since they eliminate one of the unknown variables, namely the conductivity contribution produced by solar UV and UEV radiation.

2. There should be a study to focus on making more reliable estimates of ionospheric conductances. Such a study would involve a relatively simple series of radar observations during selected times, but over a long enough period to comprise seasonal and solar cycle variations. Simultaneous data from more than one radar would be useful. The series of World Days observed by several radar facilities complemented by extra observations might be a starting point for such a study. We have already noted that the solar 10.7 cm flux may be a less suitable measure for the solar UV and EUV radiation than is believed. An improved quantitative model of the conductance produced by solar radiation with a proven activity parameter will be of general interest.

3. The peak in the SSF-derived Pedersen conductance which we often found at the poleward edge of the diffuse aurora should be investigated. It has yet to be determined whether such a peak is a typical phenomenon associated with the aurora and what physical mechanism may cause it. It is important to understand why this peak is not apparent in DMSP data.

The optimal situation would occur if several spacecraft, well instrumented and close in space and time, could be covered with radar operation while moving through the Sondrestrom field of view. Under favorable conditions such an experiment could provide a virtually 4-dimensional picture of the ionosphere, 3 dimensions in space and one in time.

REFERENCES

Banks, P. M., and G. Kockarts, *Aeronomy,* Academic Press, New York, N.Y., 1973.

Barrow, C. H., J. Watermann, D. S. Evans, and K. Wilhelm, Observations of Antarctic auroral electron precipitation with high stability in time and longitude, submitted for publication in *Ann. Geophys.,* 1990.

Barth, C. A., W. K. Tobiska, G. J. Rottman, and O. R. White, Comparison of 10.7 cm radio flux with SME solar Lyman alpha flux, *Geophys. Res. Lett., 17,* 571, 1990.

Brekke, A., and C. Hall, Auroral ionospheric quiet summer time conductances, *Annales Geophys., 6,* 361, 1988.

Cole, K. D., Eccentric Dipole Coordinates, *Aust. J. Phys., 16,* 423, 1963.

de la Beaujardière, O., R. Vondrak, and M. Baron, Radar observations of electric fields and currents associated with auroral arcs, *J. Geophys. Res., 82,* 5051, 1977.

de la Beaujardiere, O., V. Wickwar, C. Leger, M. McCready and M. Baron, The software system for the Chatanika incoherent-scatter radar, Technical Report, NSF Grant ATM 7823658, SRI project 8358, SRI International, Menlo Park, CA, November 1980.

de la Beaujardière, O., M. J. Baron, V. B. Wickwar, C Senior, and J. V. Evans, MITHRAS: A program of simultaneous radar observations of the high-latitude auroral zone, Contract Report F49620-81-C-0042, SRI International, Menlo Park, CA, 1982.

de la Beaujardiere, O., R. Johnson, V. B. Wickwar, "Ground-Based Measurements of Joule heating Rates," in press, *Proceedings of the International Conference on Auroral Physics,* Cambridge, England, 1988.

Hardy, D. A., M. S. Gussenhoven, A. Huber, The precipitating electron detectors (SSJ/3) for the block 5D/flights 2-5 DMSP satellites: Calibration and data presentation, Scientific Interim Report, AFGL-TR-79-0210, ADA 083136, SRI project 7601, Air Force Geophysics Laboratory, Hanscom Air Force Base, MA 01731, September 1979.

Hedin, A. E., A revised thermospheric model based on mass spectrometer and incoherent scatter data: MSIS-83, *J. Geophys. Res., 88,* 10170, 1983.

Mehta, N. C., Ionospheric electrodynamics and its coupling to the magnetosphere, Ph.D., thesis, University of California, San Diego, 1978.

Prolss, G. W., Magnetic storm associated perturbations of the upper atmosphere: Recent results obtained by satellite-borne gas analyzers, *Rev. Geophys. Space Phys., 18,* 183, 1980.

Rasmussen, C. E., R. W. Schunk, and V. B. Wickwar, A photochemical equilibrium model for ionospheric conductivity, *J. Geophys. Res., 93,* 9831, 1988.

Rich, F. J., Fluxgate magnetometer (SSM) for the Defense Meteorological Satellite Program (DMSP), *Air Force Geophysics Laboratory Report No. AFGL-TR-84-0225 IP,* No. 326, 1984, ADA155229.

Rich, F. J., D. A. Hardy, and M. S. Gussenhoven, Enhanced ionosphere-magnetosphere data from the DMSP satellites, *Eos, 66,* 513, 1985.

Rich, F. J., M. S. Gussenhoven, M. E. Greenspan, Using simultaneous particle and field observations on a low altitude satellite to estimate Joule heating energy flow into the high latitude ionosphere, *Annales Geophys., 5A,* 527, 1987.

Rich, F. J., M. S. Gussenhoven, D. A. Hardy, and E. Holeman, Average height-integrated Joule heating rates and magnetic deflection vectors due to field-aligned currents during sunspot minimum, submitted to *J. Atmos. Terr. Phys.,* 1989.

Robinson, R. M., and R. R. Vondrak, Measurements of E region ionization and conductivity produced by solar illumination at high latitudes, *J. Geophys. Res., 89,* 3951, 1984.

Robinson, R. M., R. R. Vondrak, K. Miller, T. Dabbs, and D. Hardy, On calculating ionospheric conductances from the flux and energy of precipitating electrons, *J. Geophys. Res., 92,* 2565, 1987.

Roble, R. G., R. E. Dickinson, and E. C. Ridley, Seasonal and solar cycle variations of the zonal mean circulation in the thermosphere, *J. Geophys. Res., 82,* 5493, 1977.

Schlegel, K., Auroral zone E-region conductivities during solar minimum derived from EISCAT data, *Annales Geophys., 6,* 129, 1988.

Senior, C., Les conductivités ionosphériques et leur rôle dans la convection magnétosphérique: Une étude expérimentale et théorique, Diplôme de docteur de 3^{e} cycle, Universite Pierre et Marie Curie, Paris, 1980.

Tsunoda, R. T., A. Q. Smith, J. D. Kelly, and R. M. Robinson, Coordinated radar and satellite studies of ionospheric currents in the auroral zone and polar cap, Final Report, Air Force Systems Command Contract F19628-82-K-0045, SRI Project 4592, SRI International, Menlo Park, CA, 1985.

Vickrey, J. F., R. R. Vondrak, and S. J. Matthews, The diurnal and latitudinal variation of auroral zone ionospheric conductivity, *J. Geophys. Res., 86,* 65, 1981.

Wallis, D. D., and E. E. Budzinski, Empirical models of height integrated conductivities, *J. Geophys. Res., 86,* 125, 1981.

PUBLISHED AND PRESENTED PAPERS SUPPORTED BY CONTRACT NO. F19628-87-K-0006

de la Beaujardière, O., Sondrestrom measurements of energy dissipation by Joule heating, paper presented at the American Geophysical Union fall meeting, 1987.

de la Beaujardière, O., Satellite and ground-based measurements of conductivities and Joule heating rates, paper presented at COSPAR Symposium, 1988.

de la Beaujardière, O., Satellite and ground-based measurements of conductivities and Joule heating rates, paper presented at Auroral Physics Conference, Cambridge, 1988.

de la Beaujardière, O., Seasonal dependence of ionospheric plasma convection, paper presented at American Geophysical Union fall meeting, 1988.

de la Beaujardière, O., and F. J. Rich, Electric fields and conductivities estimated from DMSP F7 magnetometer and particle detector data--independent validation using the Sondrestrom radar, paper presented at American Geophysical Union fall meeting, 1989.

de la Beaujardière, O., R. Johnson, and V. B. Wickwar, Ground-based measurements of Joule heating rates, in *Auroral Physics,* Cambridge University Press, in press, 1990.

de la Beaujardière, O., D. Alcaydé, J. Fontanari, C. Leger, Seasonal dependence of high-latitude electric fields, in press, *J. Geophys. Res.,* 1990.

Richmond, A. D., Y. Kamide, S. I. Akasofu, D. Alcaydé, M. Blanc, O. de la Beaujardière, D. S. Evans, J. C. Foster, E. Friis-Christensen, J. M. Holt, R. J. Pellinen, C. Senior, and A. N. Zaitzev, Global measures of ionospheric electrodynamic activity inferred from combined incoherent-scatter radar and ground magnetometer observations, *J. Geophys. Res., 95,* 1061, 1990.